Supporting Information

Efficient one-pot synthesis of *trans*-Pt(II)(salicylaldimine)(4-picoline)Cl complexes: Effective agents for enhanced expression of p53 tumor suppressor genes

Faiz-Ur-Rahman,[a] Amjad Ali,[bc] Rong Guo,[a] Wei-Kun Wang,[a] Hui Wang,*[a] Zhan-Ting Li,[a] Yuejian Lin,[a] and Dan-Wei Zhang*[a]

[a] Department of Chemistry, Fudan University, 220 Handan Road, Shanghai 200433, China.

[b] Institute of Biomedical Sciences, School of Life Sciences, East China Normal University, 500 Dongchuan Road, Shanghai 200241, China.

[c] Unit of GIGA Signal Transduction, GIGA-R, University of Liege, Tour GIGA +2 B34, Avenue de I'hopital, 1, CHU SART-Tilman 4000 Liege, Belgium

*E-mail: zhangdw@fudan.edu.cn (D.-W. Zhang), wanghui@fudan.edu.cn (H. Wang)

Tel.: +86 21 65643576

Contents

Synthesis and characterization of ligands **L1–8** 2

^{1}H, ^{13}C and ^{19}F NMR Spectra of Ligands 5

^{1}H, ^{13}C and ^{19}F NMR Spectra of platinum complexes 16

Mass Spectra of all platinum complexes 27

Stabliltiy study 31

Single crystal structure study and refinement data of **C1**, **C2** and **C3** 33

Packing plot of **C1** 34

Packing plot of **C2** 34

Packing plot of **C3** 35

Synthesis and characterization of ligands L1–8

General procedure for the synthesis of ligands L1–8

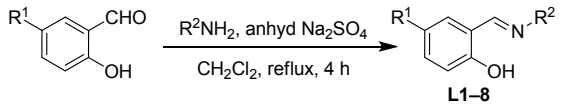

L1–8

L1: R^1 = Me, R^2 = *i*-Bu; **L2**: R^1 = Me, R^2 = Ph
L3: R^1 = Me, R^2 = 4-FPh; **L4**: R^1 = H, R^2 = Ph
L5: R^1 = H, R^2 = 4-FPh; **L6**: R^1 = F, R^2 = *i*-Bu
L7: R^1 = F, R^2 = Ph; **L8**: R^1 = F, R^2 = 4-FPh

1 mmol of amine/aniline, particular salicylaldehyde and anhyd. Na_2SO_4 (200 mg) were taken in 20 mL of CH_2Cl_2. The mixture was stirred under reflux for 4h (checked by TLC). On completion it is cooled to room temperature and filtered to remove undissolved solid which is further washed with CH_2Cl_2. The filtrate was vacuum evaporated to get **L1** to **L8** which was dried and used in the next step without further purification.

Characterization of ligand L1.

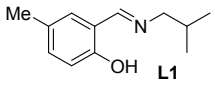

L1

Yellow liquid, ^{1}H NMR (400 MHz, $CDCl_3$) δ 13.45 (s, 1H), 8.26 (s, 1H), 7.11 (d, *J* = 8.3 Hz, 1H), 7.05 (s, 1H), 6.87 (d, *J* = 8.3 Hz, 1H), 3.41 (d, *J* = 7.5 Hz, 2H), 2.29 (s, 3H), 2.02–1.92 (m, 1H), 0.98 (d, *J* = 6.7 Hz, 6H). ^{13}C NMR (100 MHz, $CDCl_3$) δ 164.7, 159.1, 132.9, 131.2, 127.4, 118.5, 116.8, 67.6, 29.6, 20.5, 20.4.

Characterization of ligand L2.

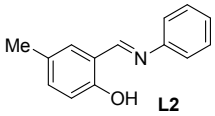

L2

Orange solid, ^{1}H NMR (400 MHz, $CDCl_3$) δ 13.01 (s, 1H), 8.56 (s, 1H), 7.41 (t, *J* = 7.7 Hz, 2H), 7.27 (t, *J* = 7.6 Hz, 3H), 7.18 (d, *J* = 7.0 Hz, 2H), 6.93 (d, *J* = 8.6 Hz, 1H), 2.31 (s, 3H). ^{13}C NMR (100 MHz, $CDCl_3$) δ 162.7, 159.0, 148.7, 134.1, 132.3, 129.4, 128.2, 126.8, 121.2, 118.9, 117.0, 20.4.

Characterization of ligand L3.

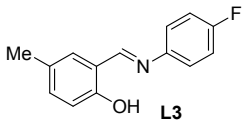

L3

Light yellow solid, ^{1}H NMR (400 MHz, $CDCl_3$) δ 12.85 (s, 1H), 8.54 (s, 1H), 7.28–7.22 (m, 2H), 7.22–7.16 (m, 2H), 7.15–7.07 (m, 2H), 6.94 (d, J = 8.1 Hz, 1H), 2.32 (s, 3H). ^{19}F NMR (376 MHz, $CDCl_3$) δ –116.17. ^{13}C NMR (100 MHz, $CDCl_3$) δ 162.5, 161.6 (d, $J_{C\text{-}F}$ = 247.45 Hz), 158.9, 144.8, 134.2, 132.3, 128.2, 122.58 (d, $J_{C\text{-}F}$ = 8.3 Hz), 118.7, 117.0, 116.2 (d, $J_{C\text{-}F}$ = 22.7 Hz), 20.4.

Characterization of ligand L4.[1]

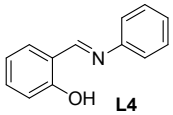

L4

Light yellow solid, ^{1}H NMR (400 MHz, $CDCl_3$) δ 13.27 (s, 1H), 8.64 (s, 1H), 7.48–7.36 (m, 4H), 7.34–7.27 (m, 3H), 7.04 (d, J = 8.1 Hz, 1H), 6.96 (t, J = 7.5 Hz, 1H). ^{13}C NMR (100 MHz, $CDCl_3$) δ 162.7, 161.2, 148.5, 133.2, 132.3, 129.4, 126.9, 121.2, 119.2, 119.1, 117.3.

Characterization of ligand L5.[2]

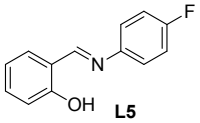

L5

Light yellow solid, ^{1}H NMR (400 MHz, $CDCl_3$) δ 13.10 (s, 1H), 8.57 (s, 1H), 7.42–7.33 (m, 2H), 7.26 (dd, J = 5.1, 3.0 Hz, 1H), 7.23 (dd, J = 5.0, 3.0 Hz, 1H), 7.15–7.06 (m, 2H), 7.02 (d, J = 8.8 Hz, 1H), 6.94 (t, J = 7.5 Hz, 1H). ^{19}F NMR (376 MHz, $CDCl_3$) δ –115.93. ^{13}C NMR (100 MHz, $CDCl_3$) δ 162.5, 161.7 (d, $J_{C\text{-}F}$ = 247.45 Hz), 161.1, 160.4, 144.7, 133.2, 132.3, 122.6 (d, $J_{C\text{-}F}$ = 8.3 Hz), 119.2, 117.3, 116.2 (d, $J_{C\text{-}F}$ = 22.7 Hz).

Characterization of ligand L6.

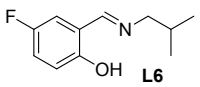

L6

Yellow liquid, ^{1}H NMR (400 MHz, $CDCl_3$) δ 13.41 (s, 1H), 8.25 (s, 1H), 7.06–6.98 (m, 1H), 6.95 (dd, J = 8.4, 3.1 Hz, 1H), 6.90 (dd, J = 9.0, 4.5 Hz, 1H), 3.43 (d, J = 6.5 Hz, 2H), 2.03–1.93 (m, 1H), 0.98 (d, J = 6.7 Hz, 6H). ^{19}F NMR (376 MHz, $CDCl_3$) δ –

126.64. ^{13}C NMR (100 MHz, $CDCl_3$) δ 163.7, 157.4, 155.3 (d, $J_{C\text{-}F}$ = 236.2 Hz), 119.0 (d, $J_{C\text{-}F}$ = 23.2 Hz), 118.5 (d, $J_{C\text{-}F}$ = 7.2 Hz), 118.0 (d, $J_{C\text{-}F}$ = 7.4 Hz), 116.2 (d, $J_{C\text{-}F}$ = 23.1 Hz), 67.6, 29.6, 20.4.

Characterization of ligand L7.

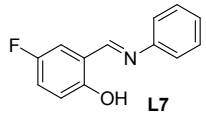

L7

Orange solid, ^{1}H NMR (400 MHz, $CDCl_3$) δ 13.02 (s, 1H), 8.56 (s, 1H), 7.49–7.38 (m, 2H), 7.36–7.26 (m, 3H), 7.16–7.05 (m, 2H), 7.02–6.94 (m, 1H). ^{19}F NMR (376 MHz, $CDCl_3$) δ –125.82. ^{13}C NMR (100 MHz, $CDCl_3$) δ 161.5, 157.3, 155.6 (d, $J_{C\text{-}F}$ = 237.5 Hz), 148.1, 129.5, 127.3, 121.2, 120.3 (d, $J_{C\text{-}F}$ = 23.3 Hz), 118.9 (d, $J_{C\text{-}F}$ = 6.8 Hz), 118.4 (d, $J_{C\text{-}F}$ = 7.3 Hz), 117.1 (d, $J_{C\text{-}F}$ = 23.2 Hz).

Characterization of ligand L8.[3]

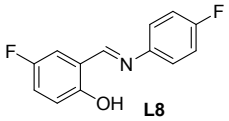

L8

Orange solid, ^{1}H NMR (400 MHz, $CDCl_3$) δ 12.87 (s, 1H), 8.53 (s, 1H), 7.33–7.22 (m, 2H), 7.18–7.05 (m, 4H), 6.98 (dd, J = 8.7, 4.5 Hz, 1H). ^{19}F NMR (376 MHz, $CDCl_3$) δ –115.27, –125.68. ^{13}C NMR (100 MHz, $CDCl_3$) δ 161.9 (d, $J_{C\text{-}F}$ = 248.5 Hz), 161.2, 157.2, 155.6 (d, $J_{C\text{-}F}$ = 237.4 Hz), 144.3, 122.7 (d, $J_{C\text{-}F}$ = 8.4 Hz), 120.35 (d, $J_{C\text{-}F}$ = 23.3 Hz), 118.8 (d, $J_{C\text{-}F}$ = 5.7 Hz), 118.4 (d, $J_{C\text{-}F}$ = 7.4 Hz), 117.1 (d, $J_{C\text{-}F}$ = 23.1 Hz), 116.4 (d, $J_{C\text{-}F}$ = 22.8 Hz).

References:

1. X. Ni, Z. Liang, J. Ling, X. Li and Z. Shen, *Polym. Int.*, 2011, **60**, 1745.
2. D.-P. Song, Y.-G. Li, R. Lu, N.-H. Hu and Y.-s. Li, *Appl. Organomet. Chem.*, 2008, **22**, 333.
3. L. Shi, R. Q. Fang, Z. W. Zhu, Y. Yang, K. Cheng, W. Q. Zhong and H. L. Zhu, *Eur. J. Med. Chem.*, 2010, **45**, 4358.

^{1}H, ^{13}C and ^{19}F NMR Spectra of Ligands

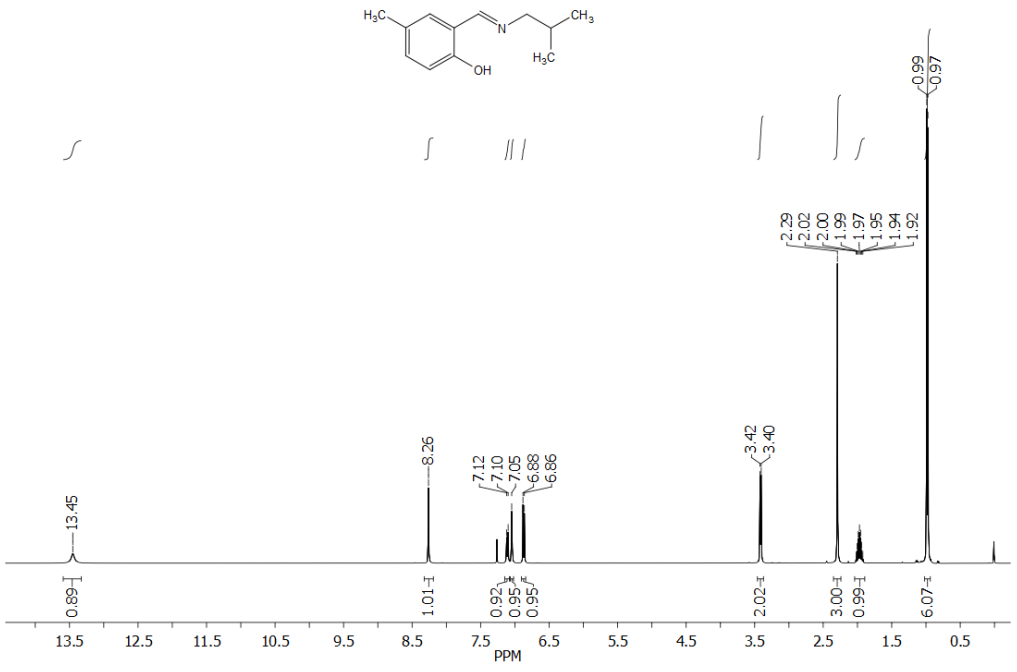

Fig. S1 ^{1}H NMR of **L1** in $CDCl_3$ at 25°C

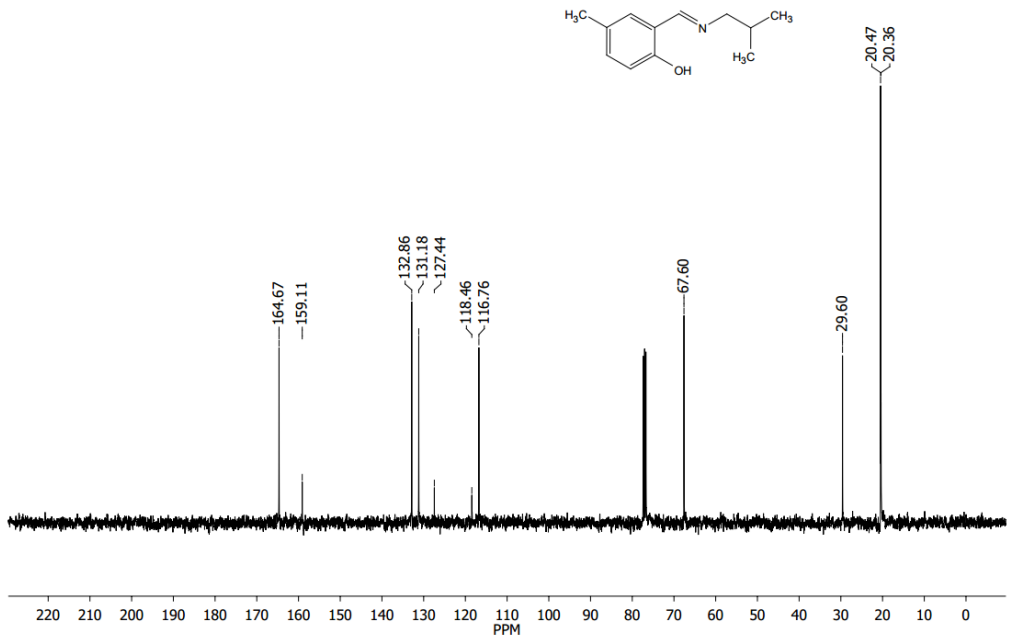

Fig. S2 ^{13}C NMR of **L1** in $CDCl_3$ at 25°C

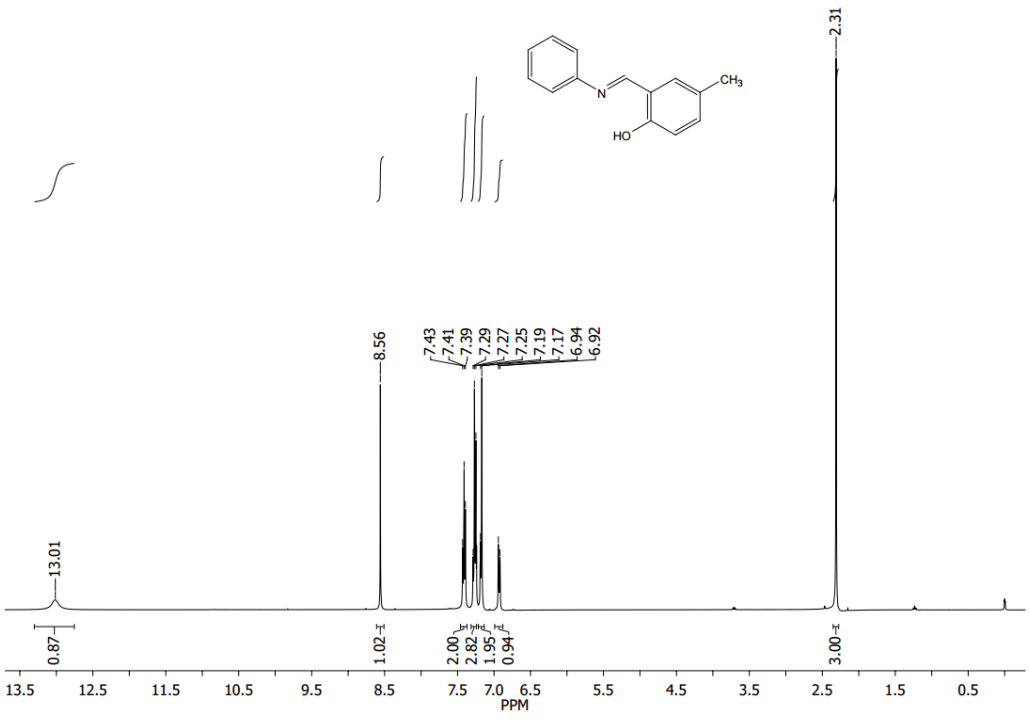

Fig. S3 ^{1}H NMR of **L2** in $CDCl_3$ at 25°C

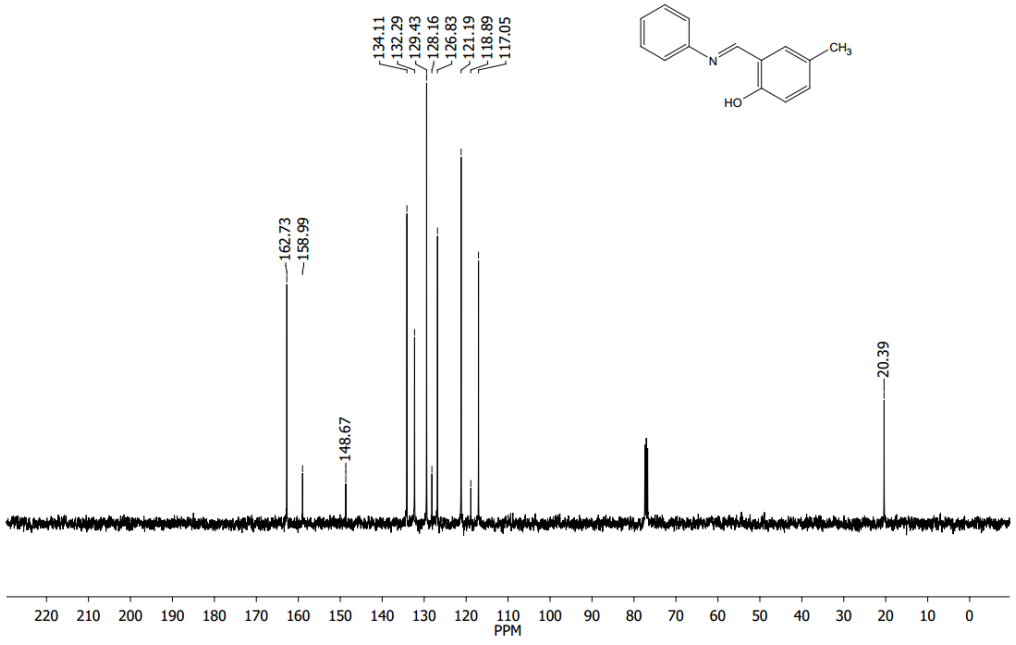

Fig. S4 ^{13}C NMR of **L2** in $CDCl_3$ at 25°C

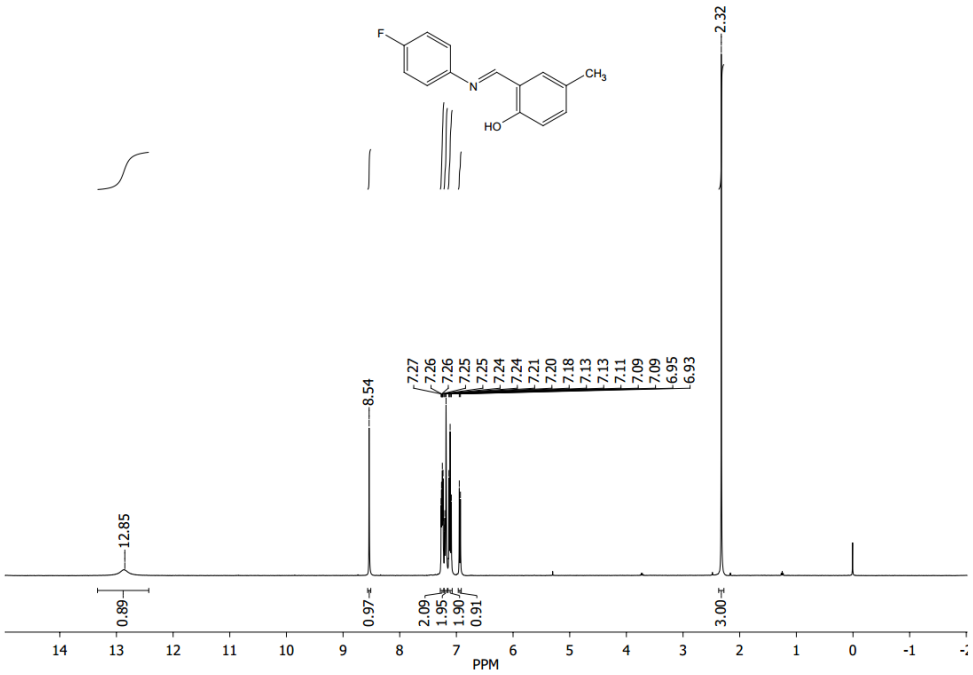

Fig. S5 ^{1}H NMR of **L3** in $CDCl_3$ at 25°C

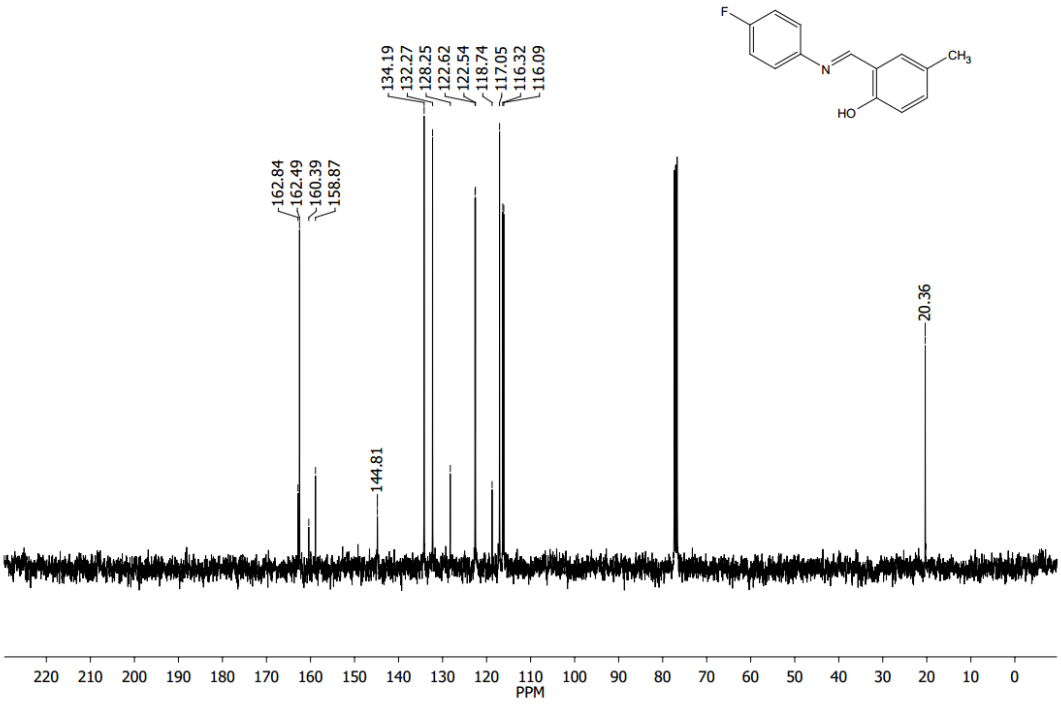

Fig. S6 ^{13}C NMR of **L3** in $CDCl_3$ at 25°C

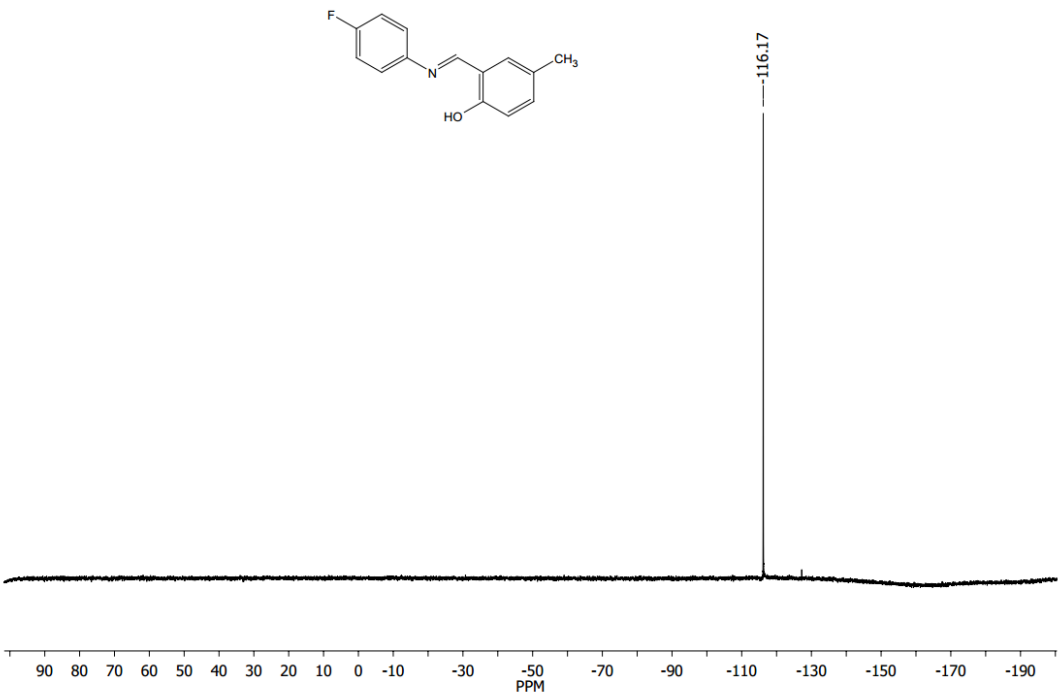

Fig. S7 ^{19}F NMR of **L3** in $CDCl_3$ at 25°C

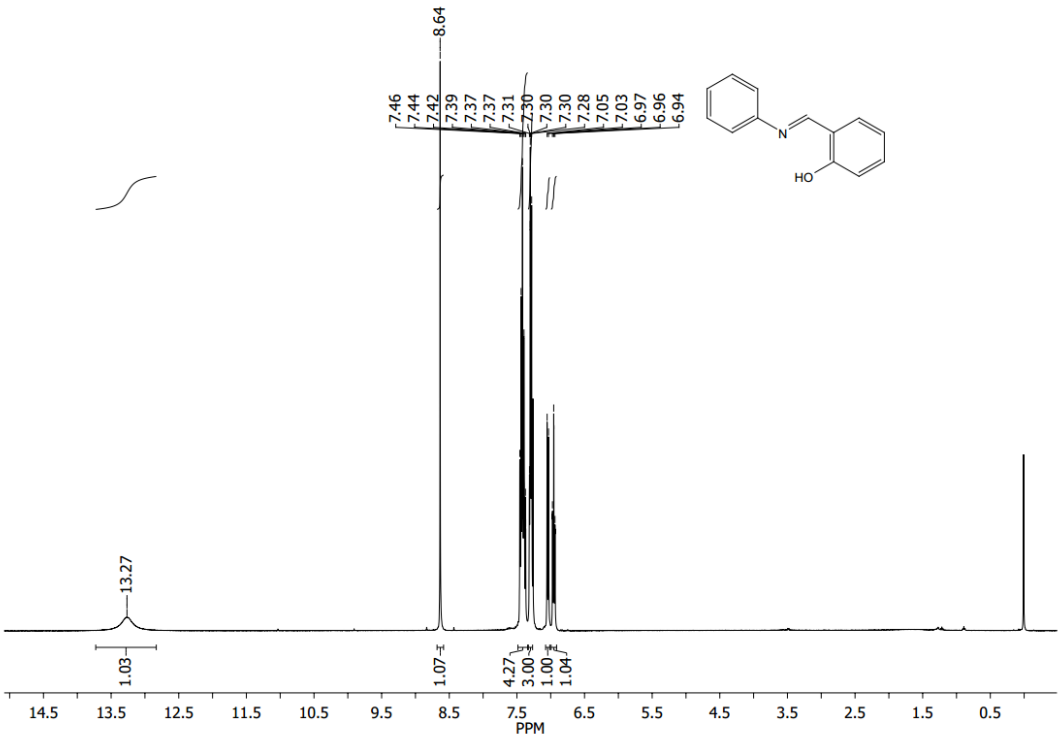

Fig. S8 ^{1}H NMR of **L4** in $CDCl_3$ at 25°C

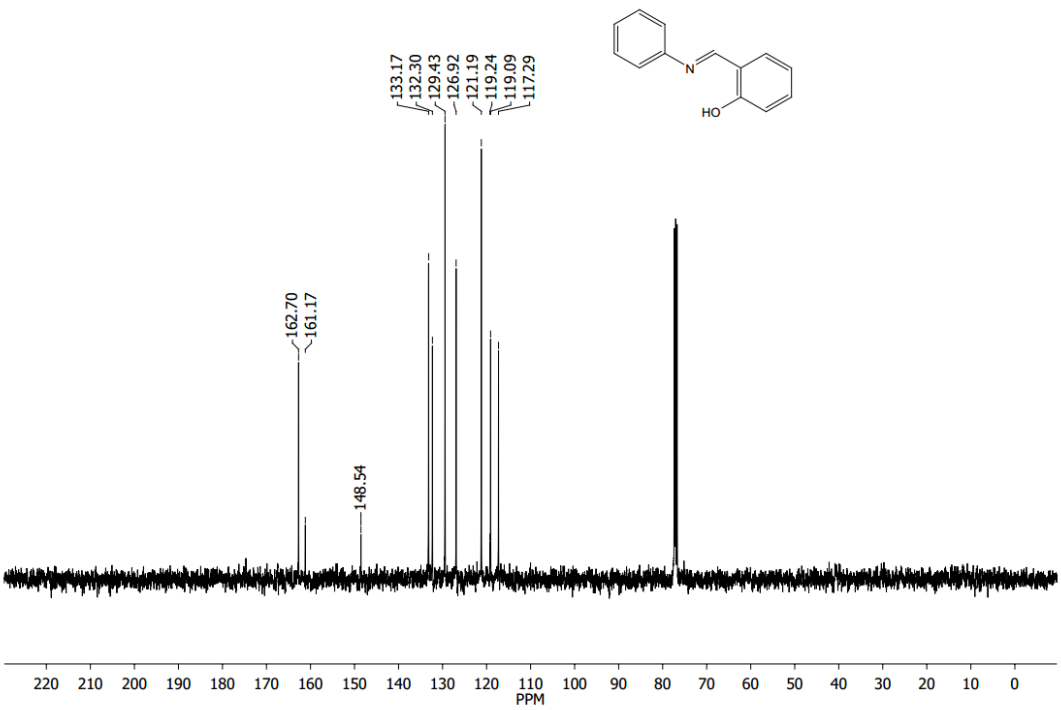

Fig. S9 ^{13}C NMR of **L4** in $CDCl_3$ at 25°C

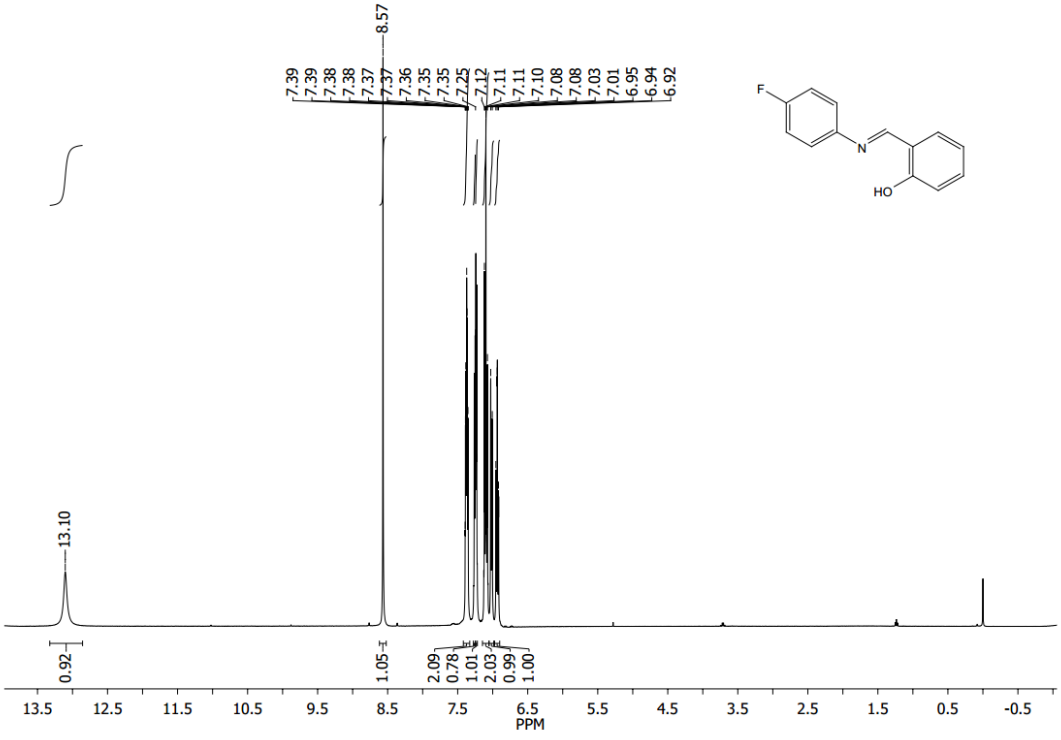

Fig. S10 ^{1}H NMR of **L5** in $CDCl_3$ at 25°C

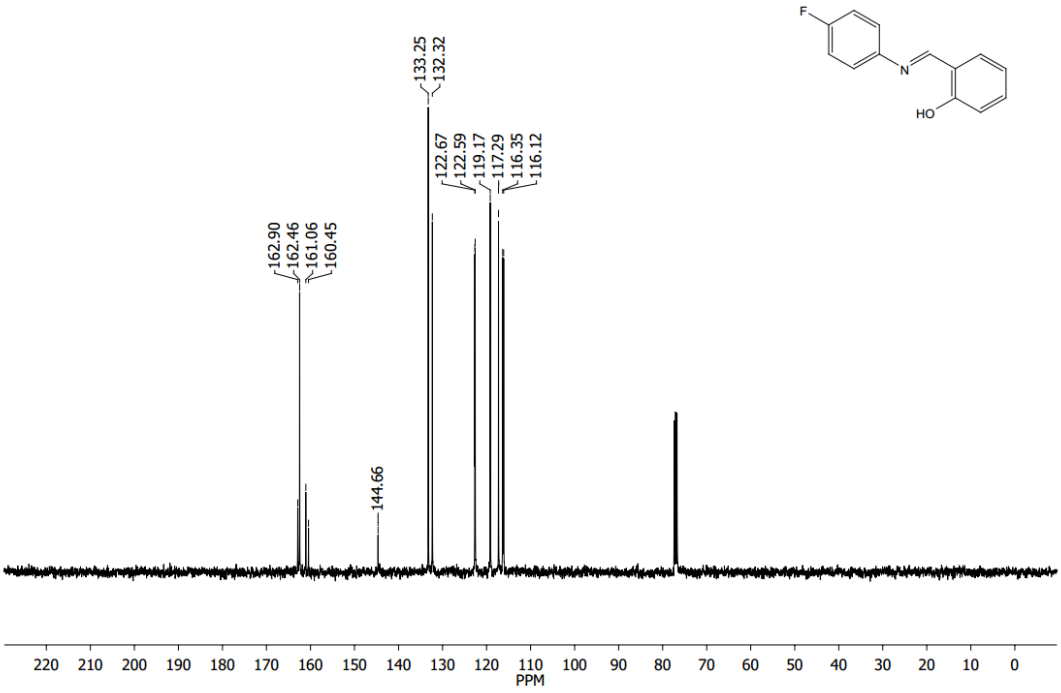

Fig. S11 ^{13}C NMR of **L5** in $CDCl_3$ at 25°C

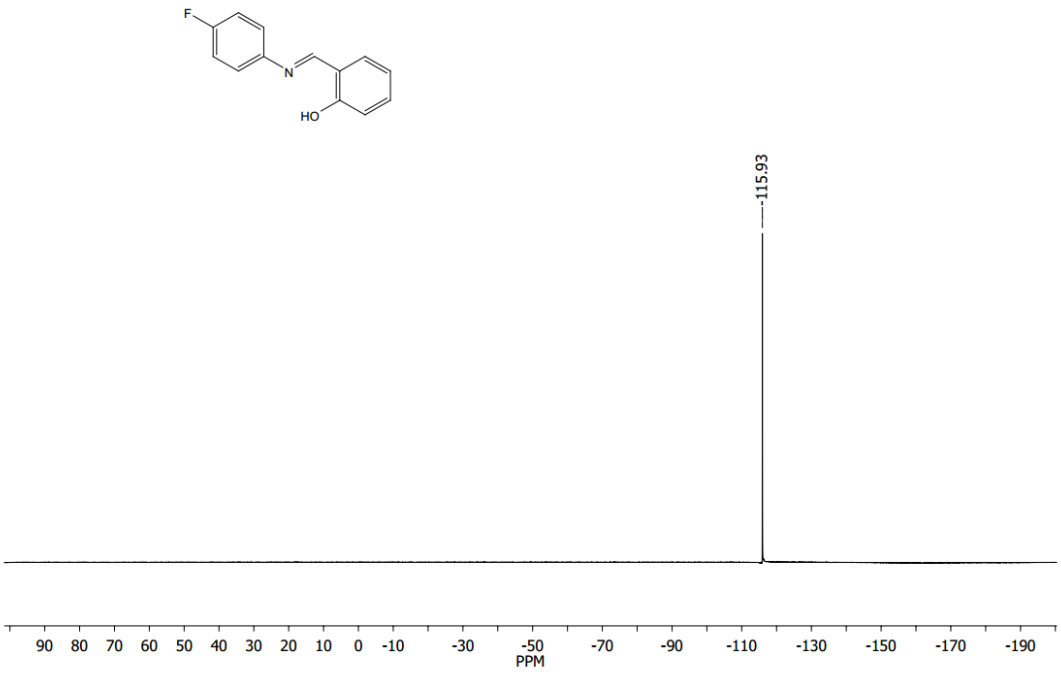

Fig. S12 ^{19}F NMR of **L5** in $CDCl_3$ at 25°C

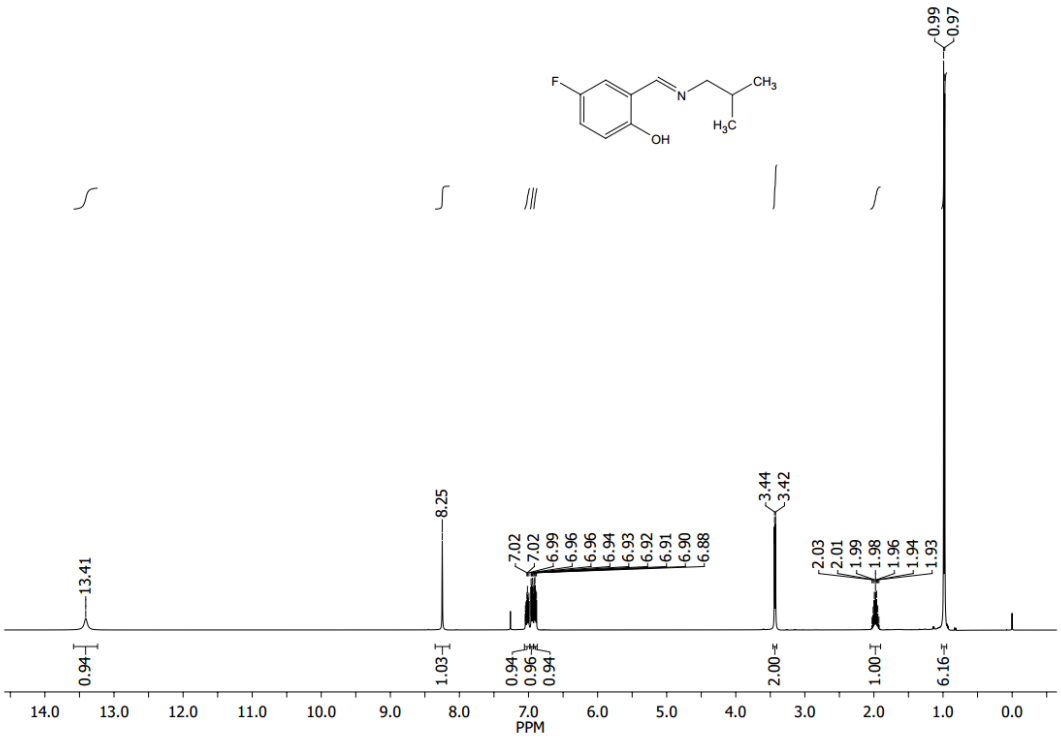

Fig. S13 ^{1}H NMR of **L6** in $CDCl_3$ at 25°C

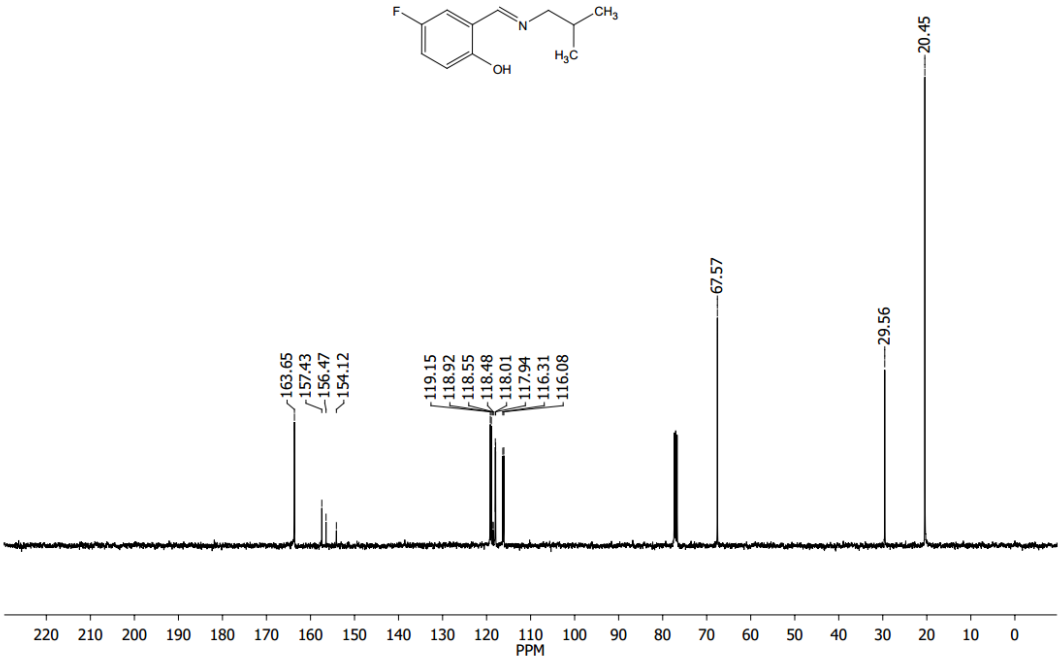

Fig. S14 ^{13}C NMR of **L6** in $CDCl_3$ at 25°C

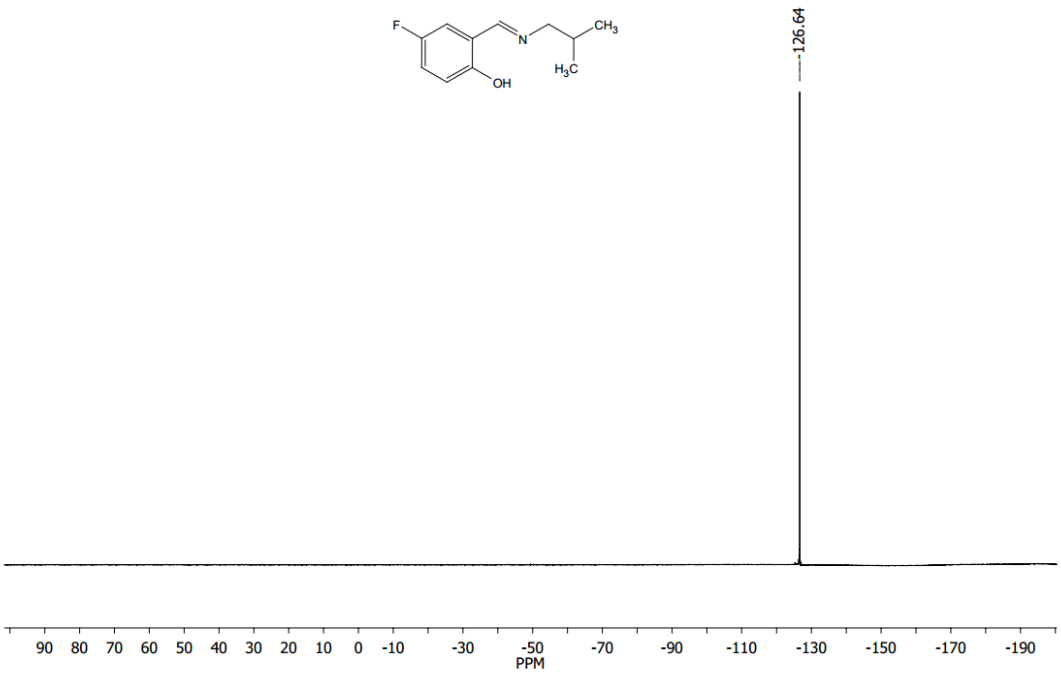

Fig. S15 ^{19}F NMR of **L6** in $CDCl_3$ at 25°C

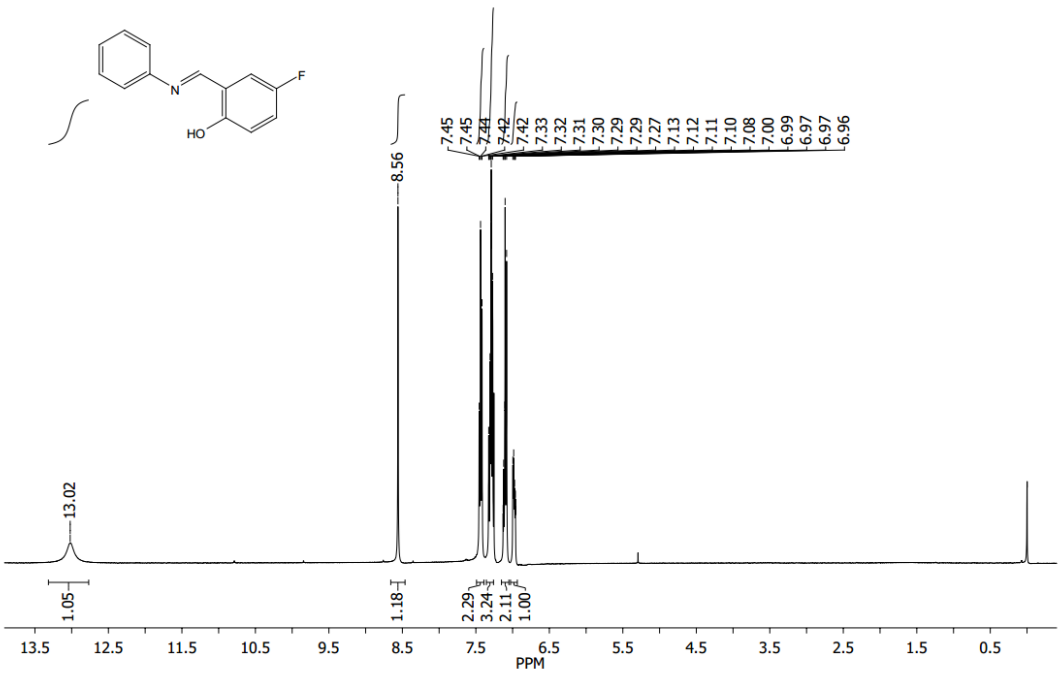

Fig. S16 ^{1}H NMR of **L7** in $CDCl_3$ at 25°C

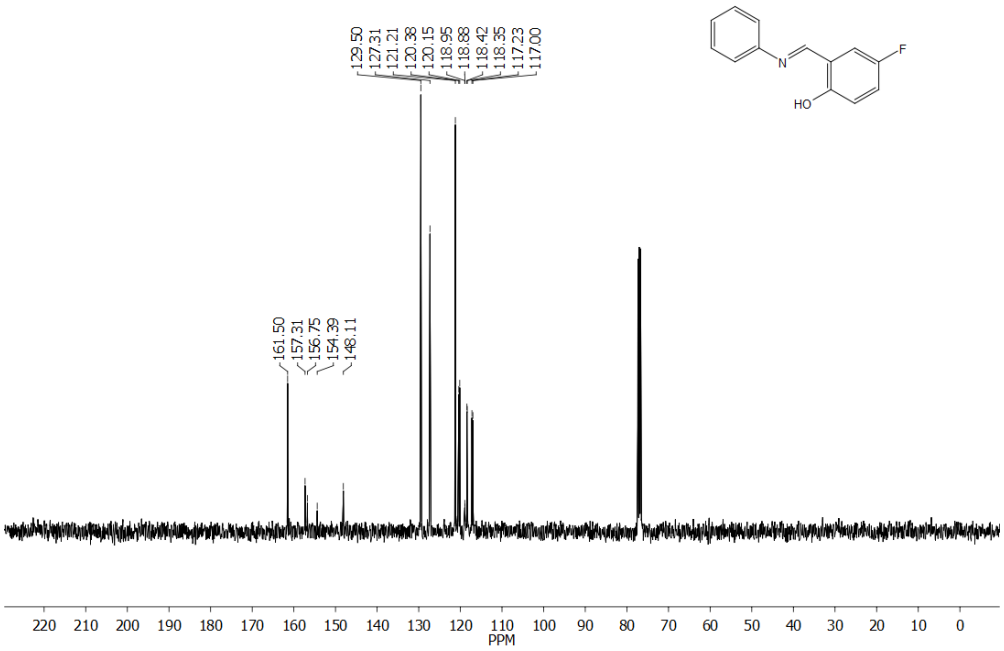

Fig. S17 ^{13}C NMR of **L7** in $CDCl_3$ at 25°C

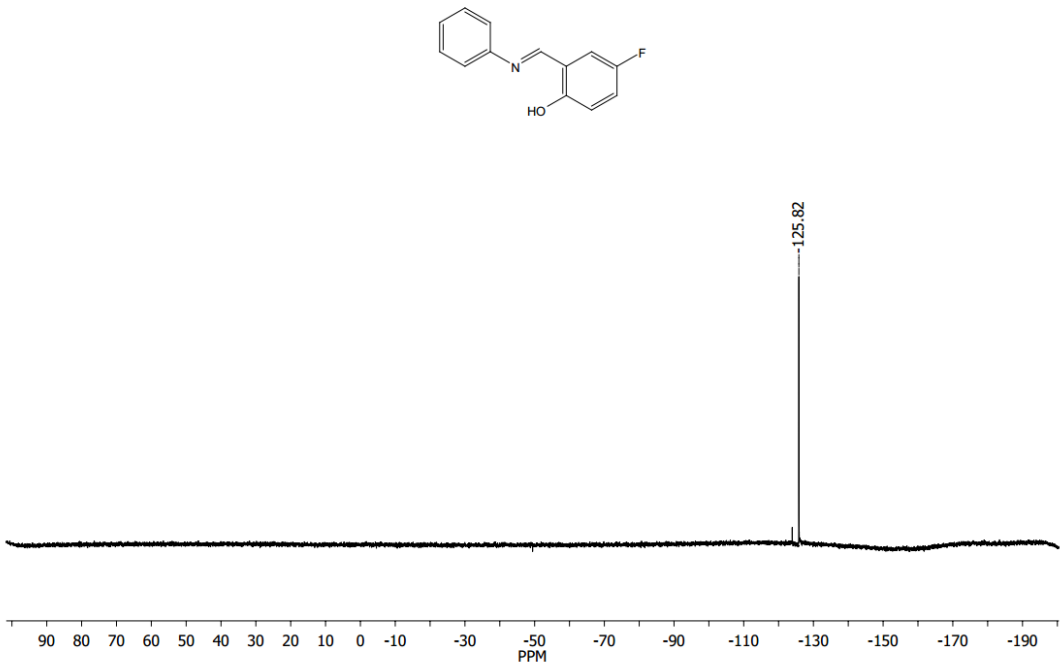

Fig. S18 ^{19}F NMR of **L7** in $CDCl_3$ at 25°C

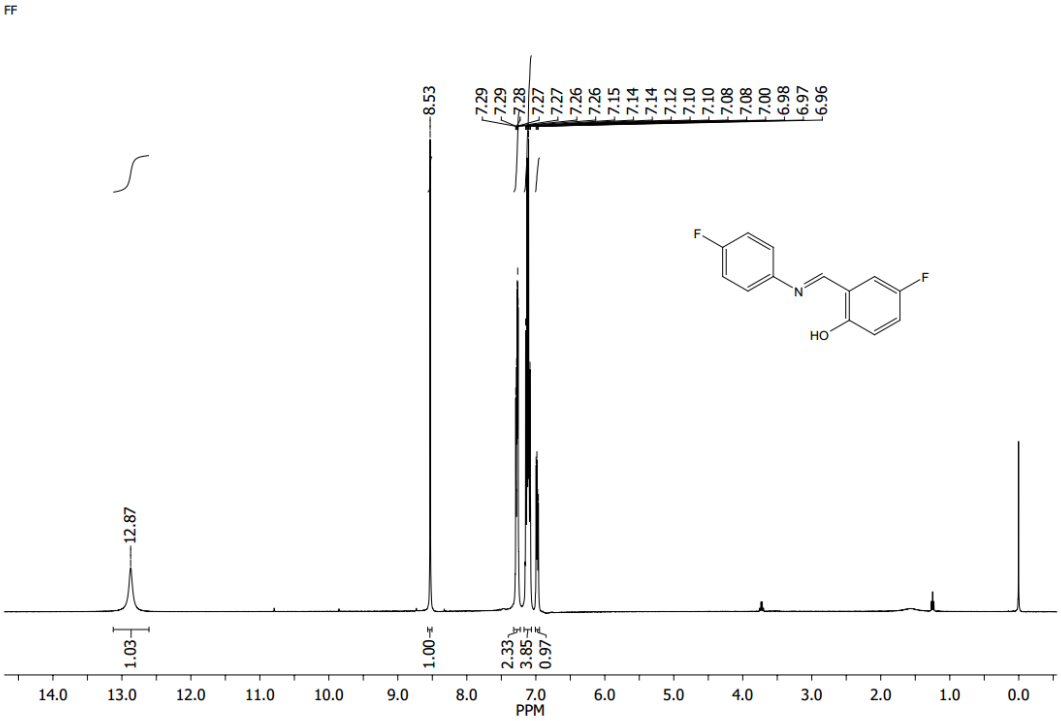

Fig. S19 ^{1}H NMR of **L8** in $CDCl_3$ at 25°C

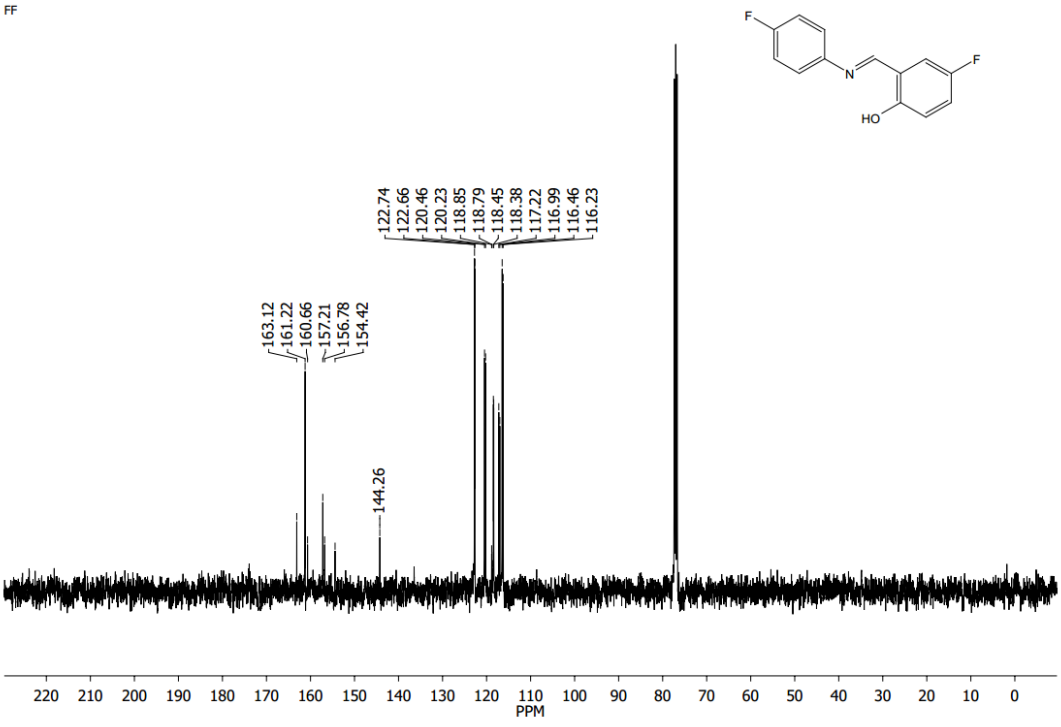

Fig. S20 ^{13}C NMR of **L8** in $CDCl_3$ at 25°C

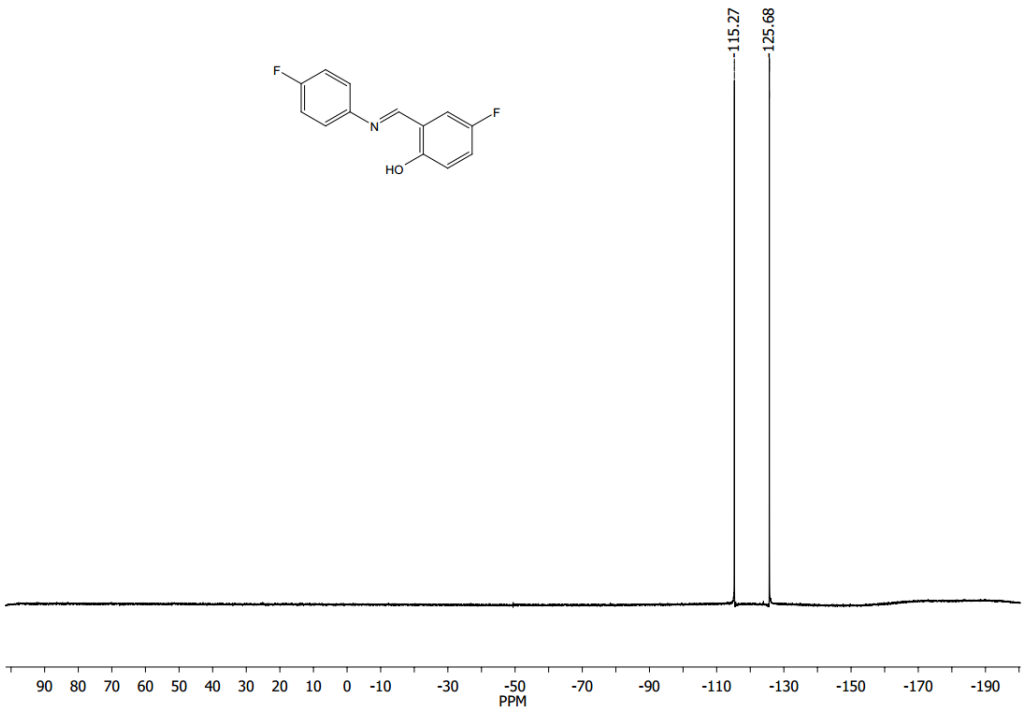

Fig. S21 ^{19}F NMR of **L8** in $CDCl_3$ at 25°C

^{1}H, ^{13}C and ^{19}F NMR Spectra of platinum complexes

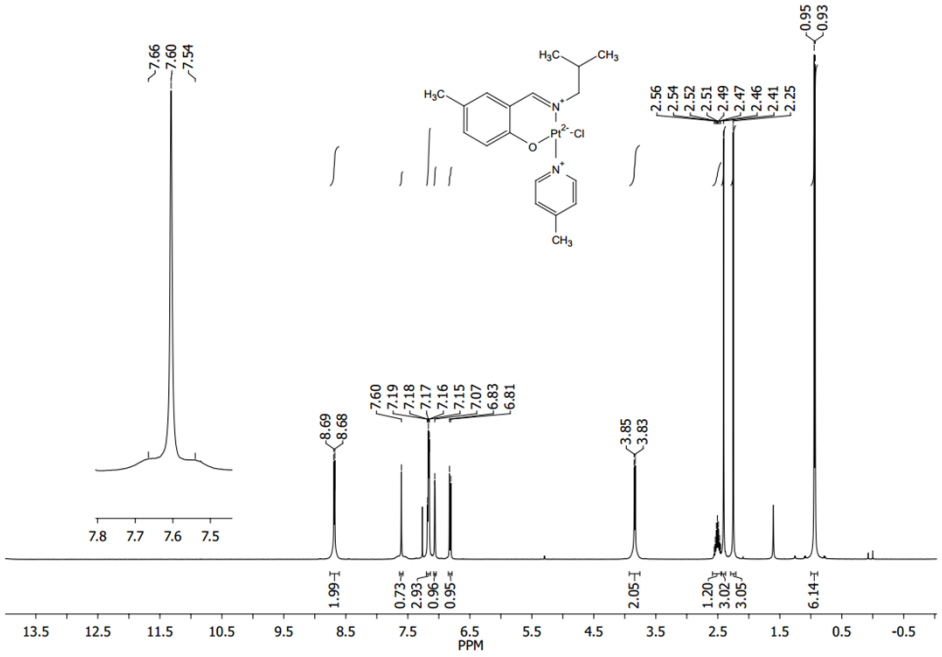

Fig. S22 ^{1}H NMR of **C1** in $CDCl_3$ at 25°C

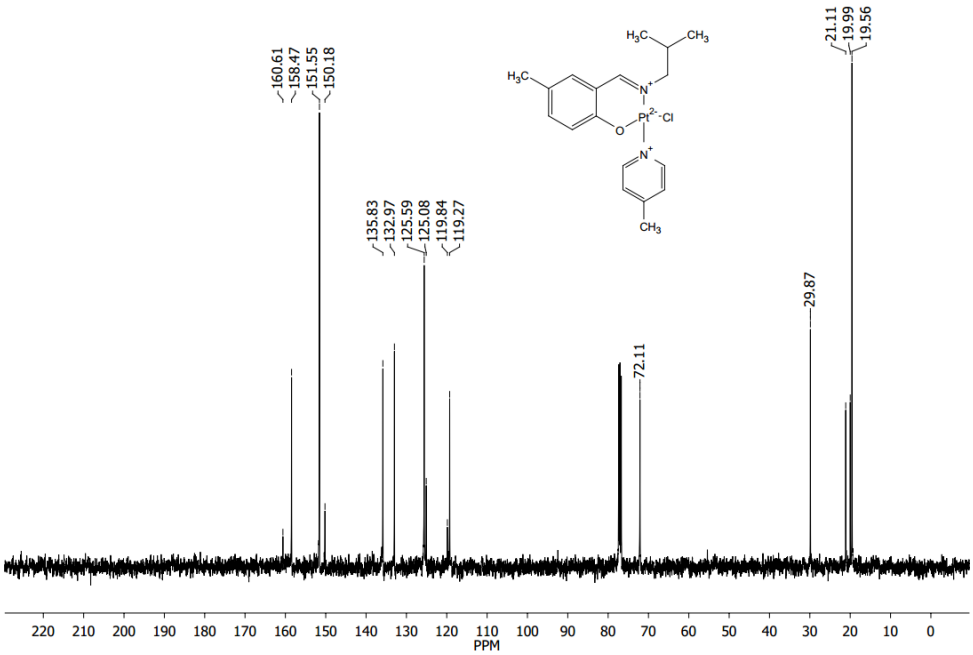

Fig. S23 ^{13}C NMR of **C1** in $CDCl_3$ at 25°C

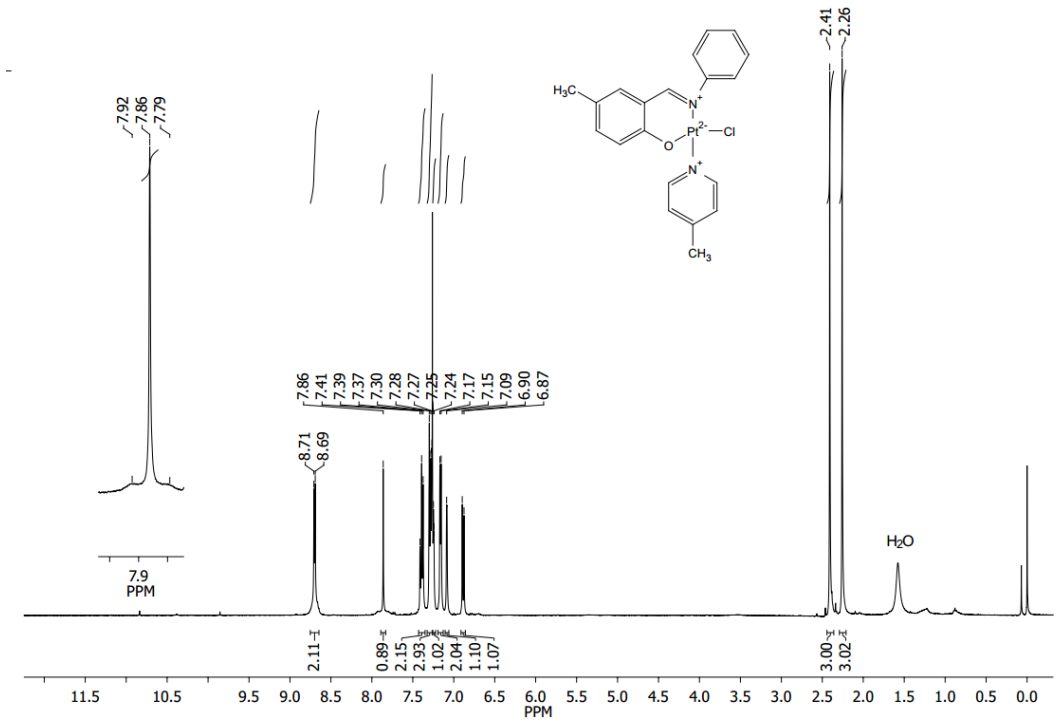

Fig. S24 ^{1}H NMR of **C2** in $CDCl_3$ at 25°C

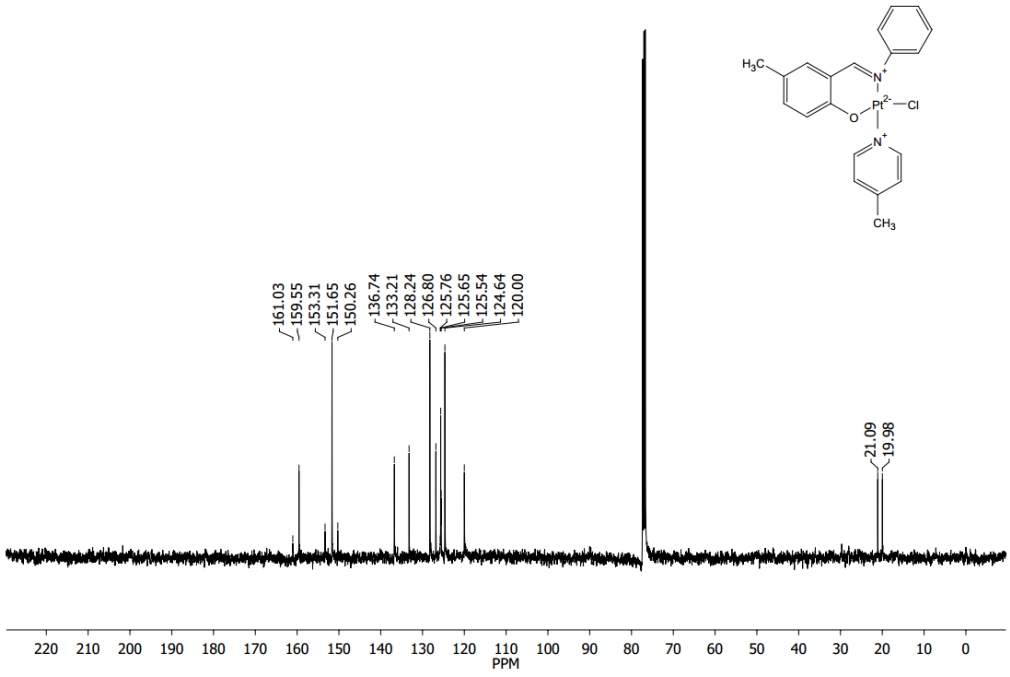

Fig. S25 ^{13}C NMR of **C2** in $CDCl_3$ at 25°C

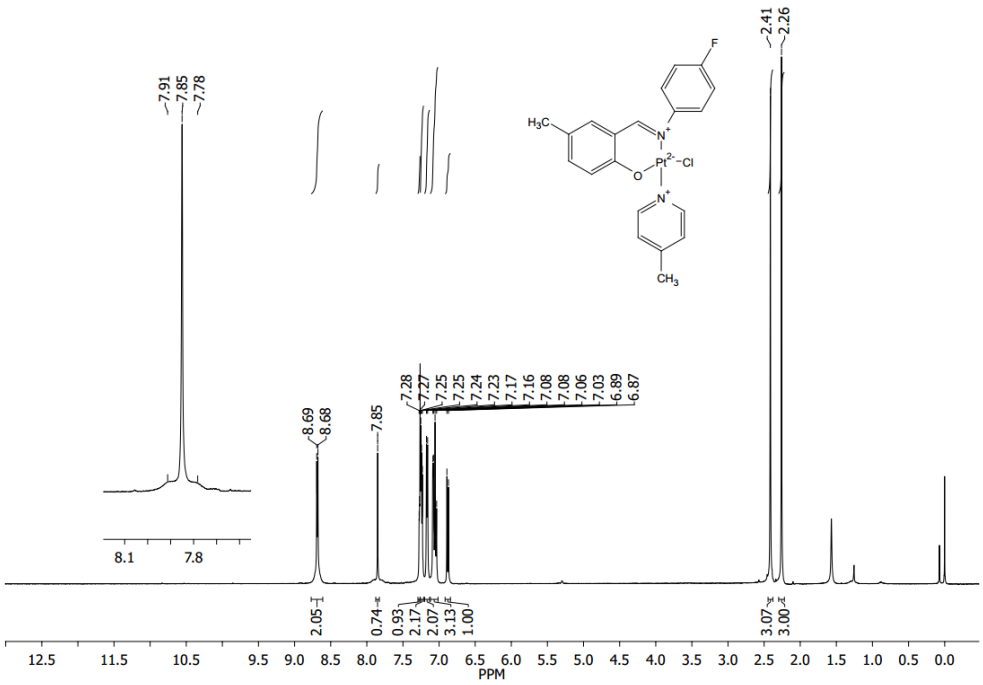

Fig. S26 ^{1}H NMR of **C3** in $CDCl_3$ at 25°C

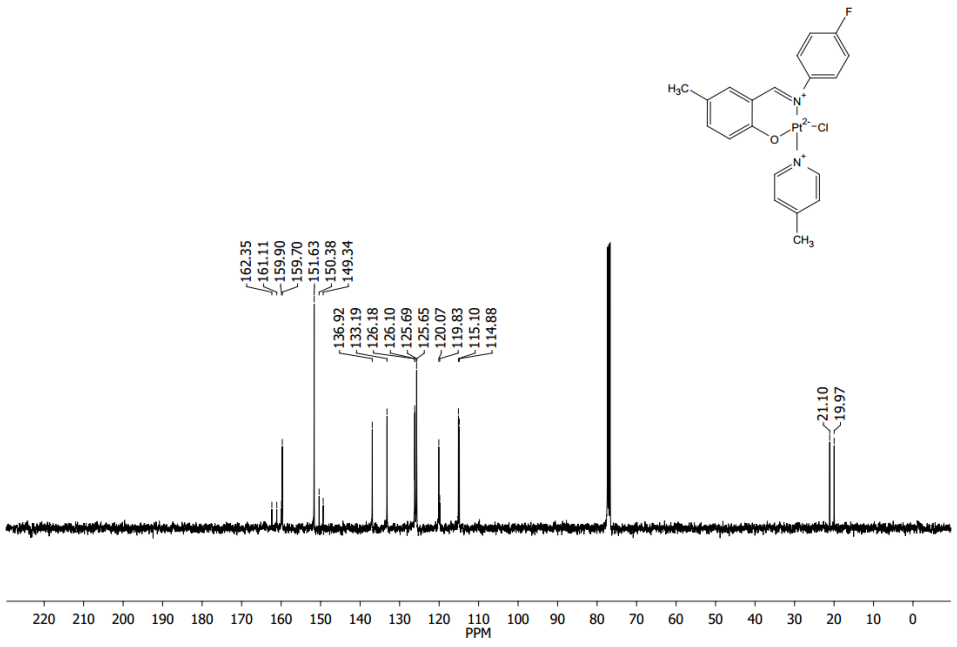

Fig. S27 ^{13}C NMR of **C3** in $CDCl_3$ at 25°C

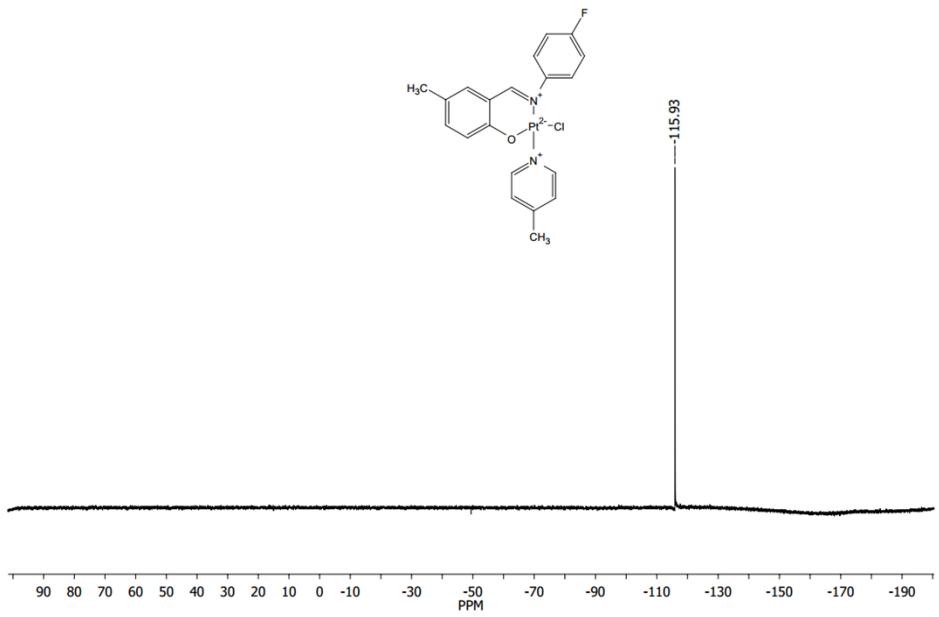

Fig. S28 ^{19}F NMR of **C3** in $CDCl_3$ at 25°C

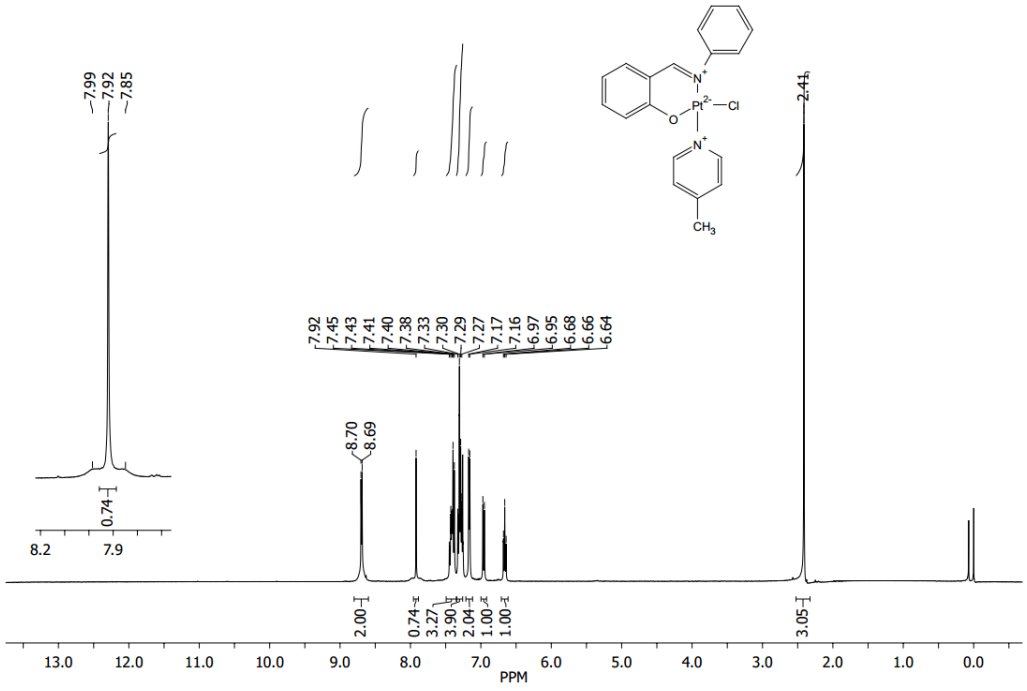

Fig. S29 ^{1}H NMR of **C4** in $CDCl_3$ at 25°C

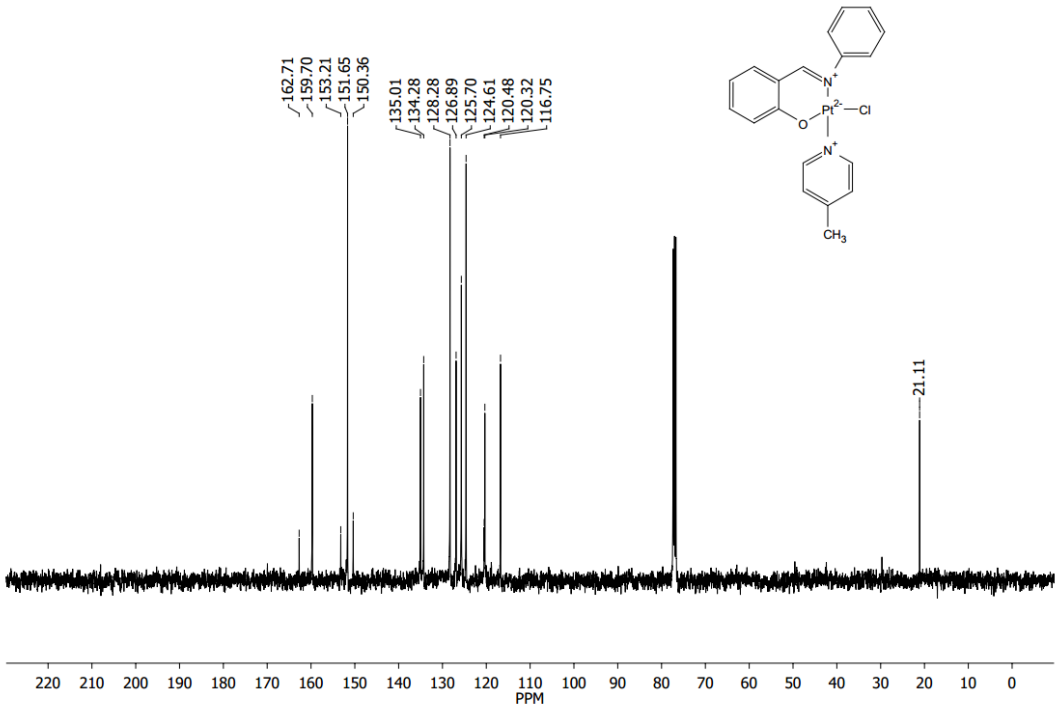

Fig. S30 ^{13}C NMR of **C4** in $CDCl_3$ at 25°C

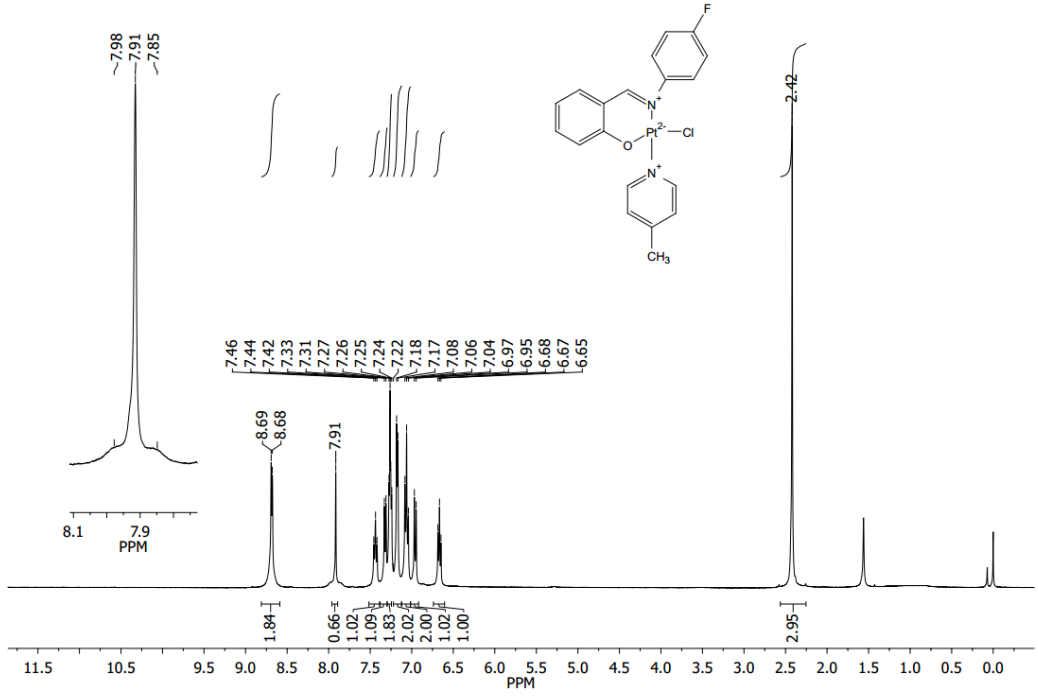

Fig. S31 ^{1}H NMR of **C5** in $CDCl_3$ at 25°C

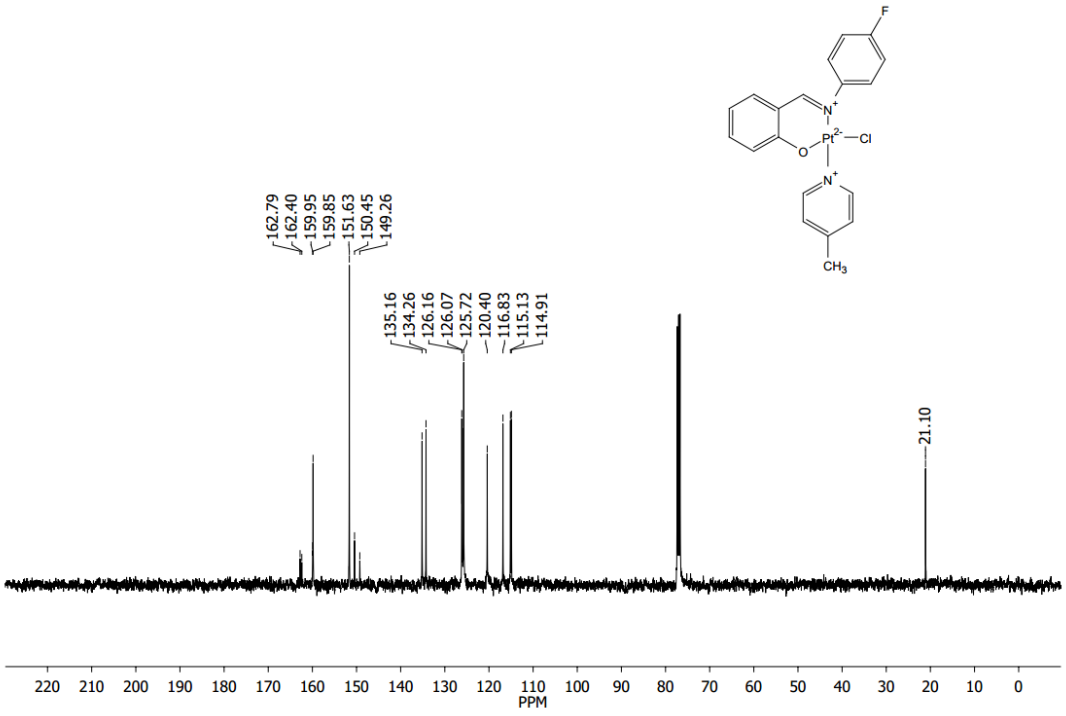

Fig. S32 ^{13}C NMR of **C5** in $CDCl_3$ at 25°C

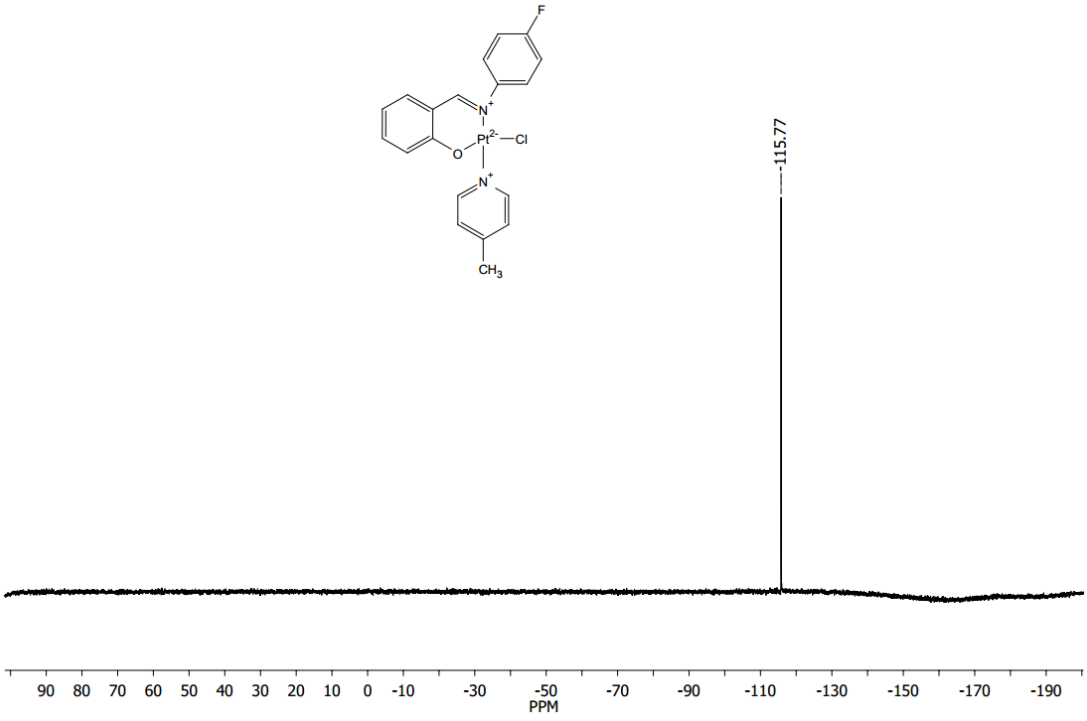

Fig. S33 ^{19}F NMR of **C5** in $CDCl_3$ at 25°C

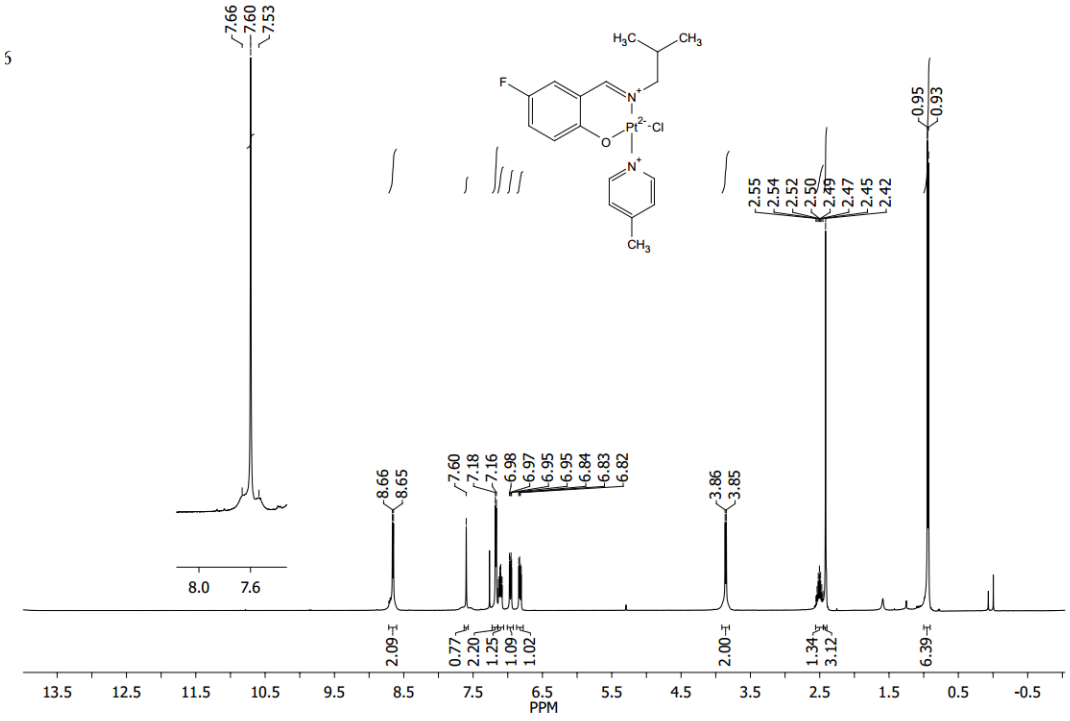

Fig. S34 ^{1}H NMR of **C6** in $CDCl_3$ at 25°C

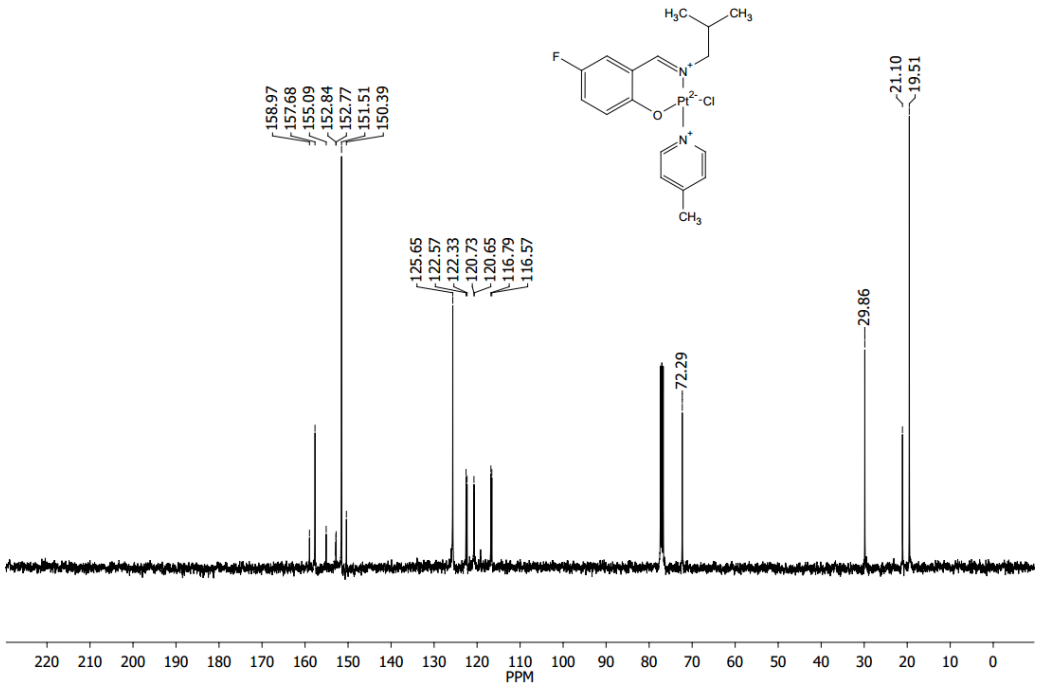

Fig. S35 ^{13}C NMR of **C6** in $CDCl_3$ at 25°C

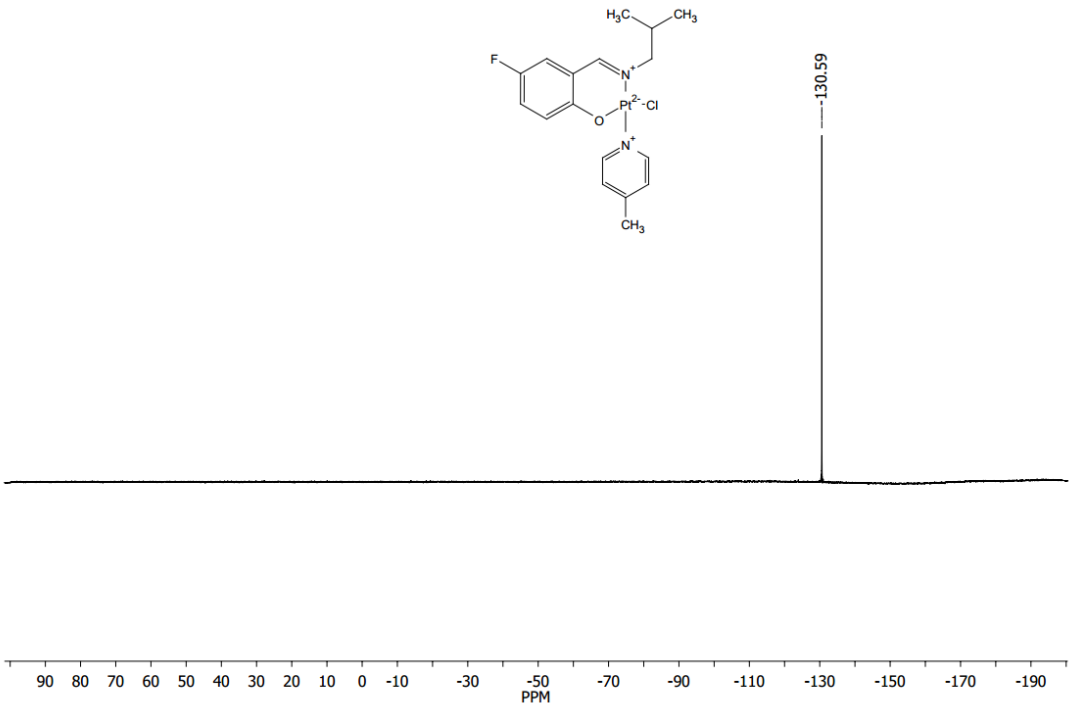

Fig. S36 ^{19}F NMR of **C6** in $CDCl_3$ at 25°C

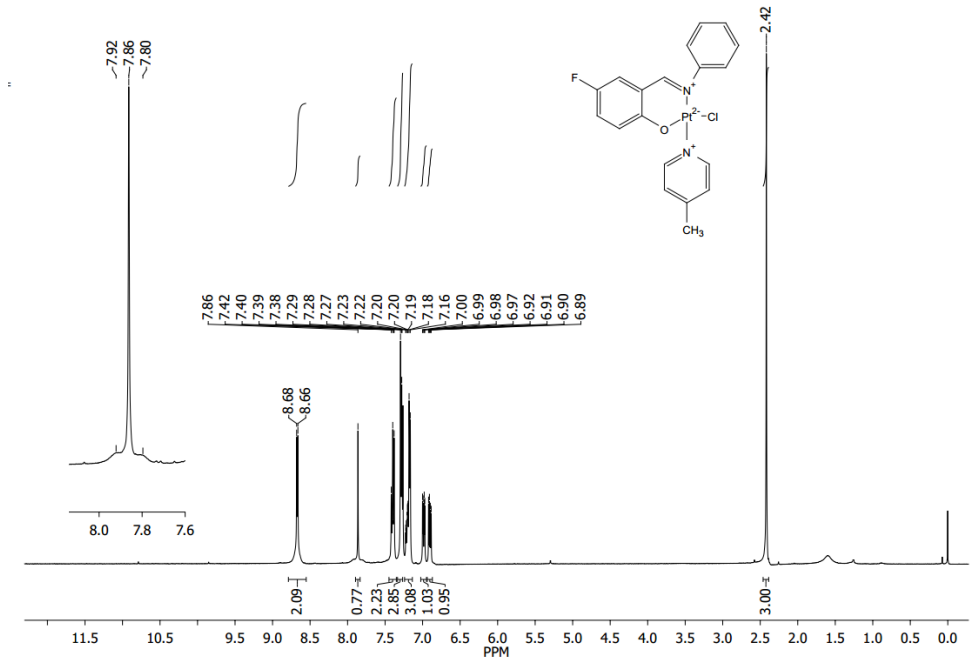

Fig. S37 ^{1}H NMR of **C7** in $CDCl_3$ at 25°C

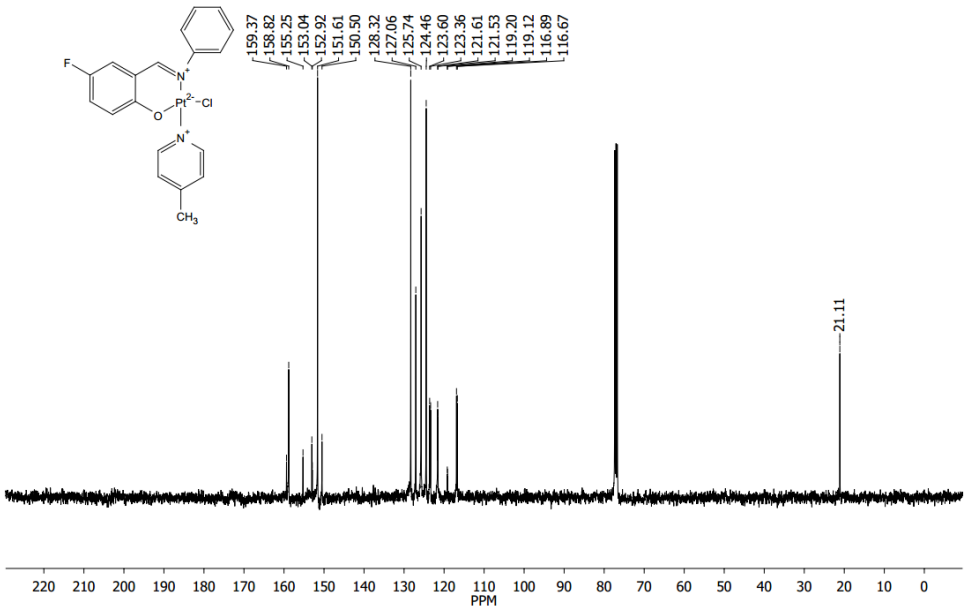

Fig. S38 ^{13}C NMR of **C7** in $CDCl_3$ at 25°C

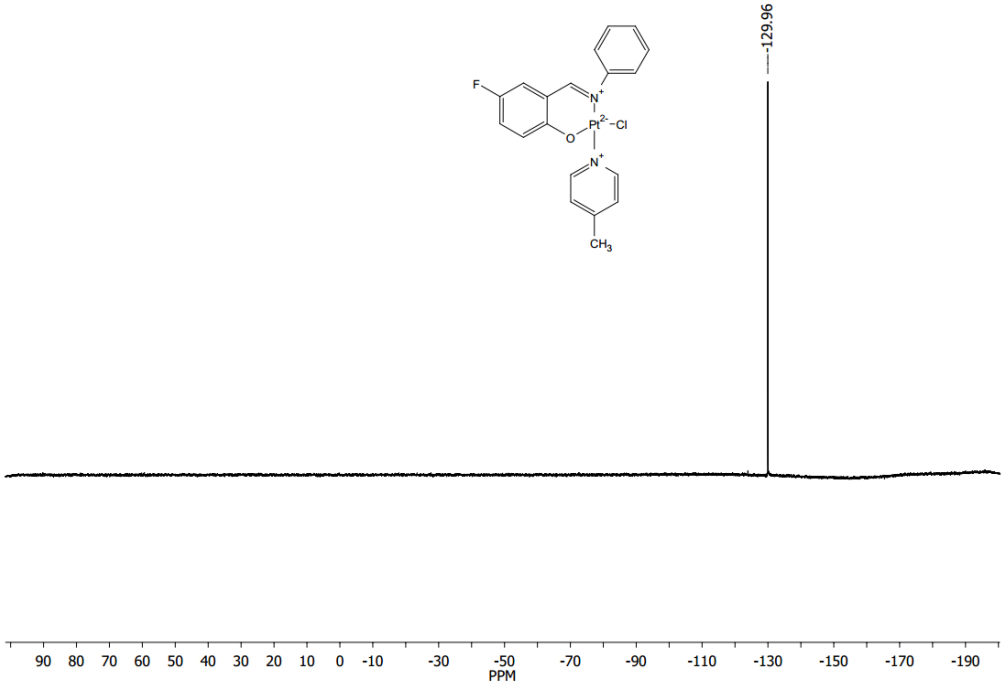

Fig. S39 ^{19}F NMR of **C7** in $CDCl_3$ at 25°C

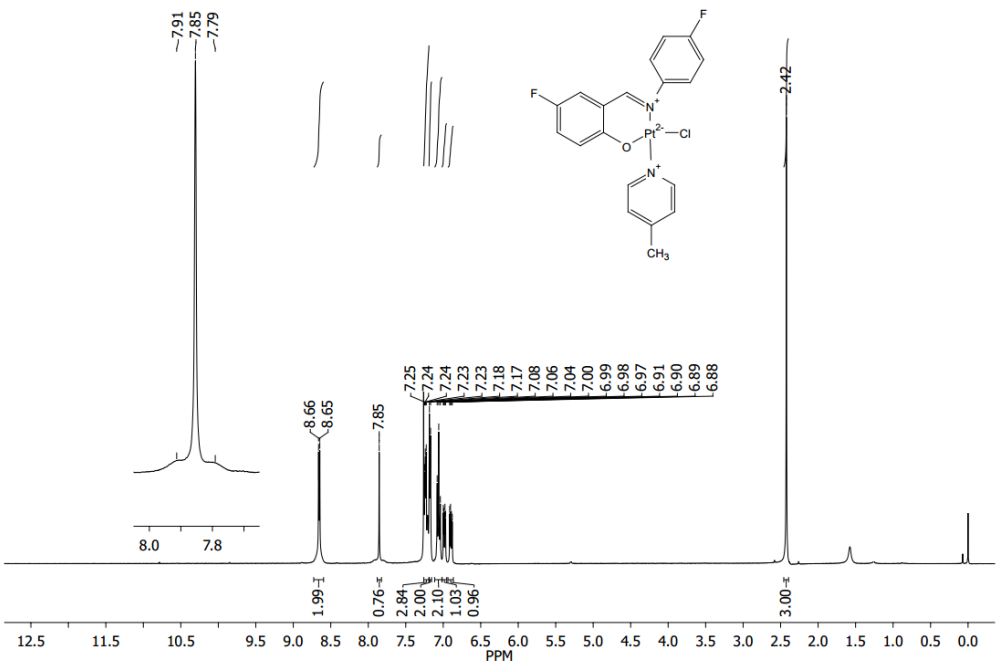

Fig. S40 ^{1}H NMR of **C8** in $CDCl_3$ at 25°C

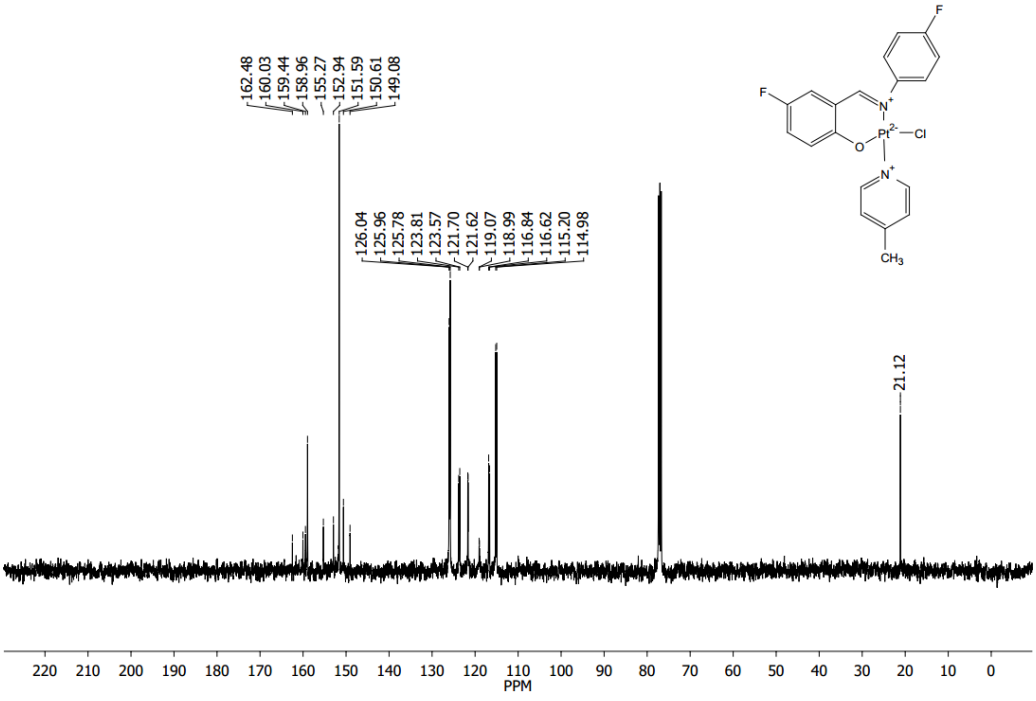

Fig. S41 ^{13}C NMR of **C8** in $CDCl_3$ at 25°C

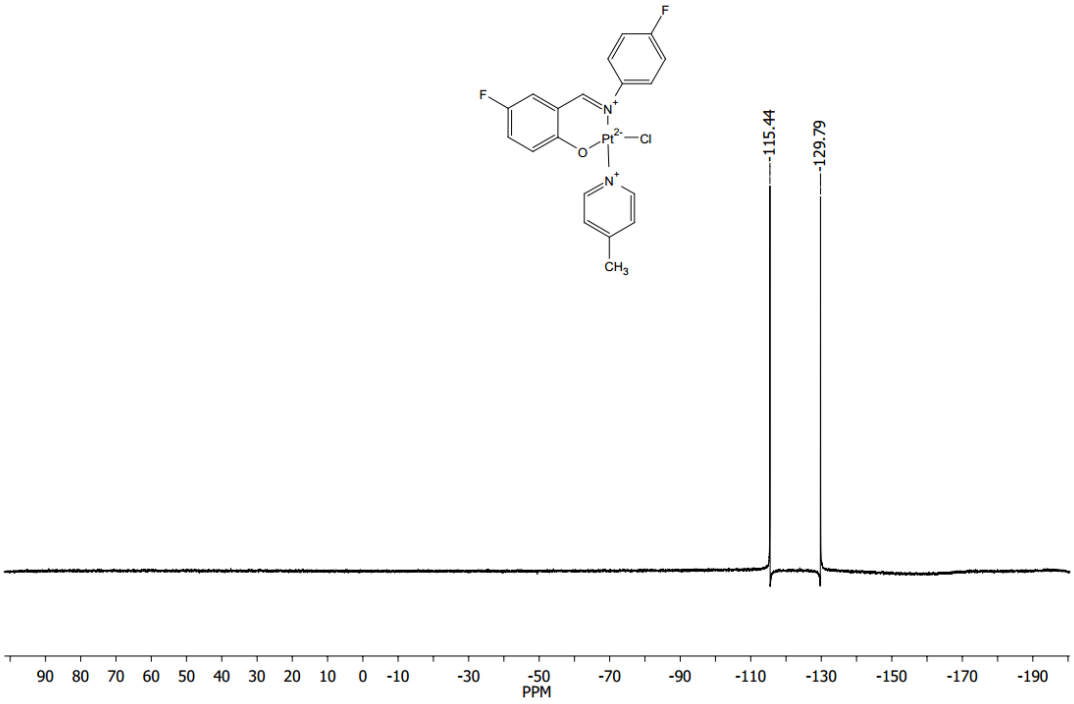

Fig. S42 ^{19}F NMR of **C8** in $CDCl_3$ at 25°C

Mass Spectra of all platinum complexes

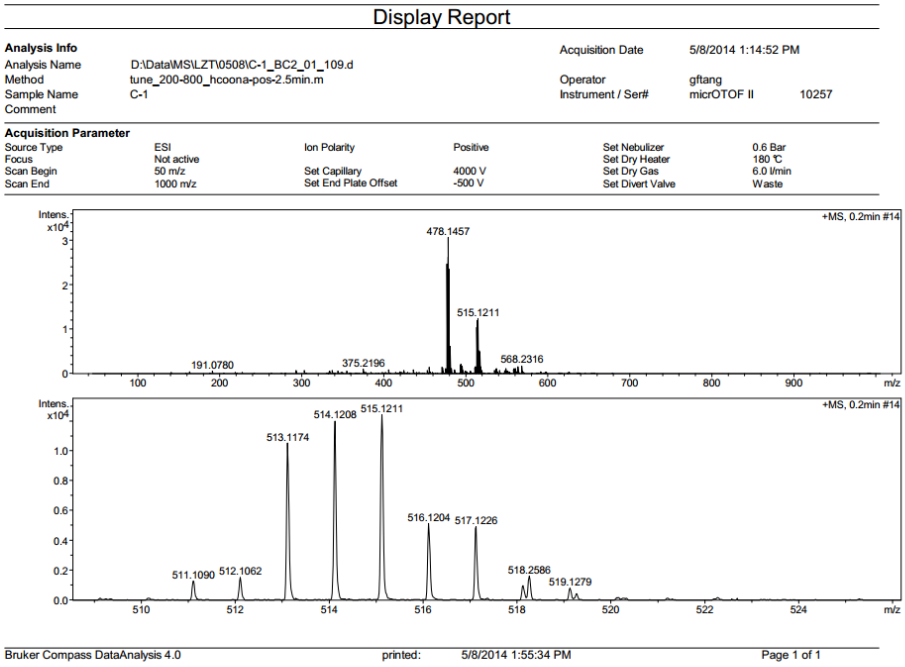

Fig. S43 Mass Spectrum of **C1**

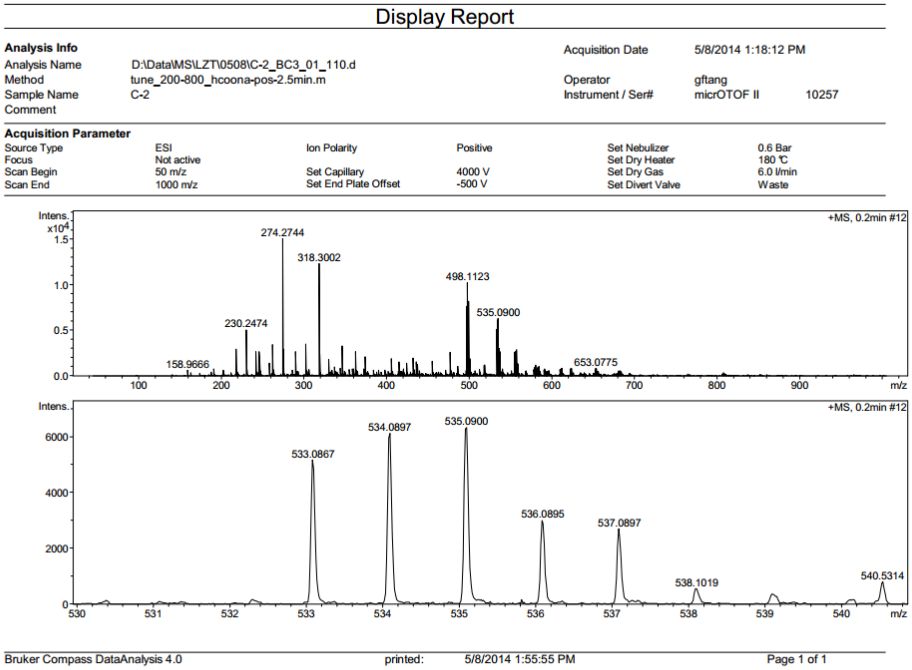

Fig. S44 Mass Spectrum of **C2**

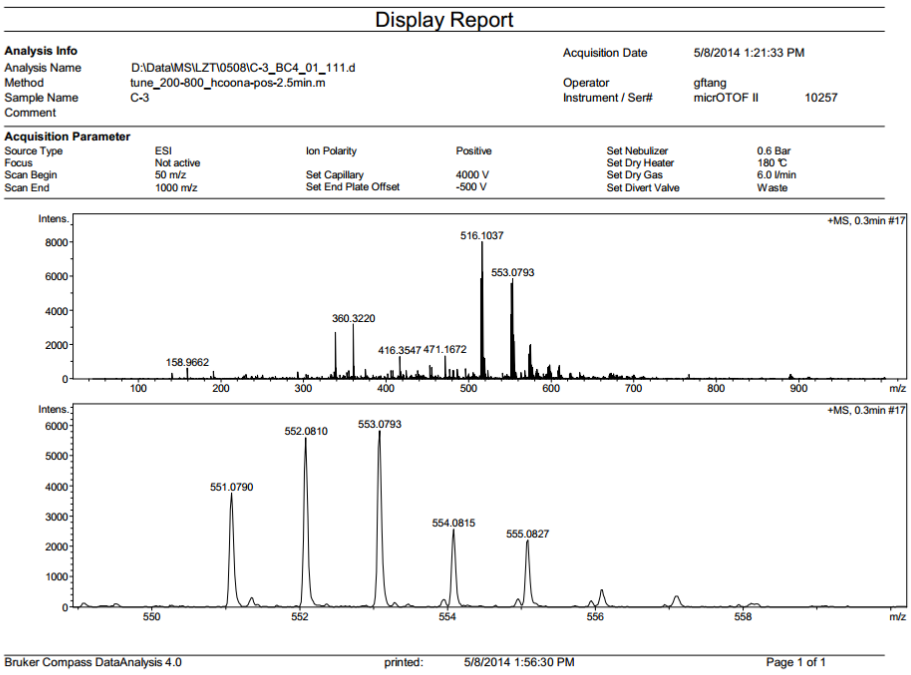

Fig. S45 Mass Spectrum of **C3**

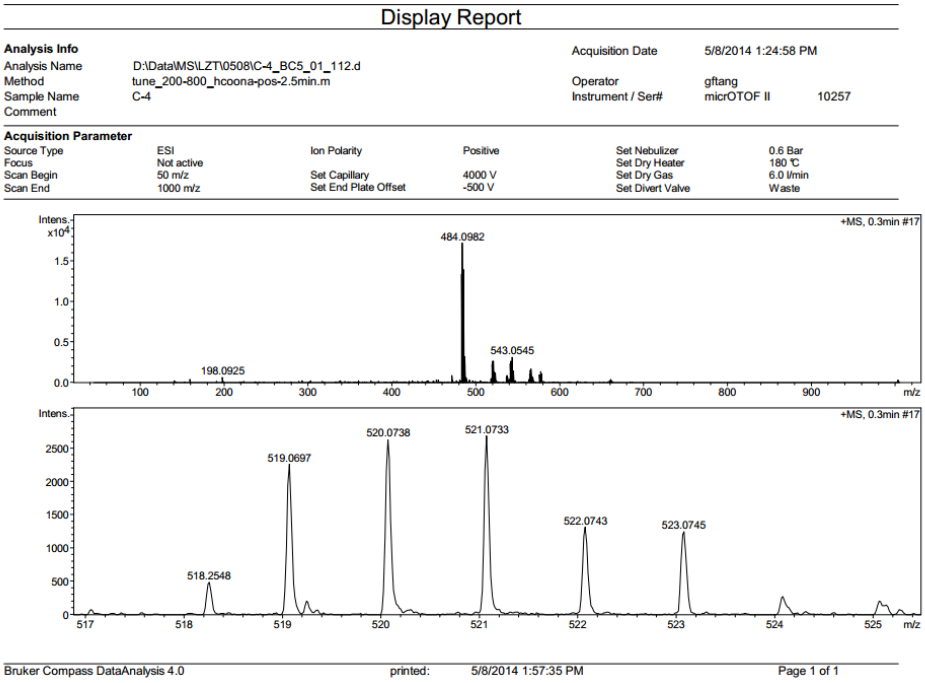

Fig. S46 Mass Spectrum of **C4**

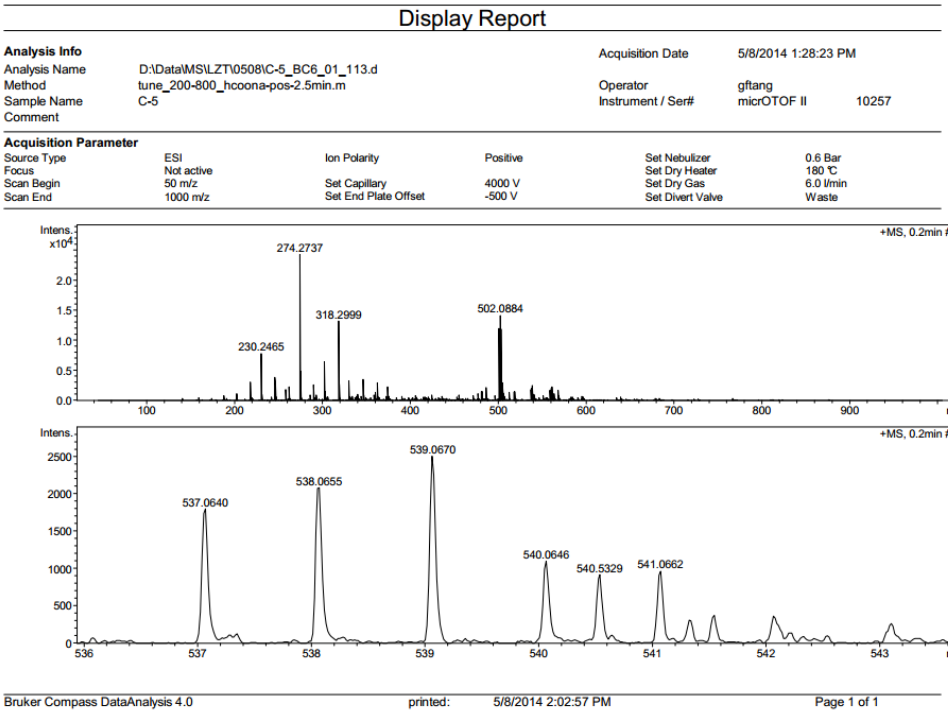

Fig. S47 Mass Spectrum of **C5**

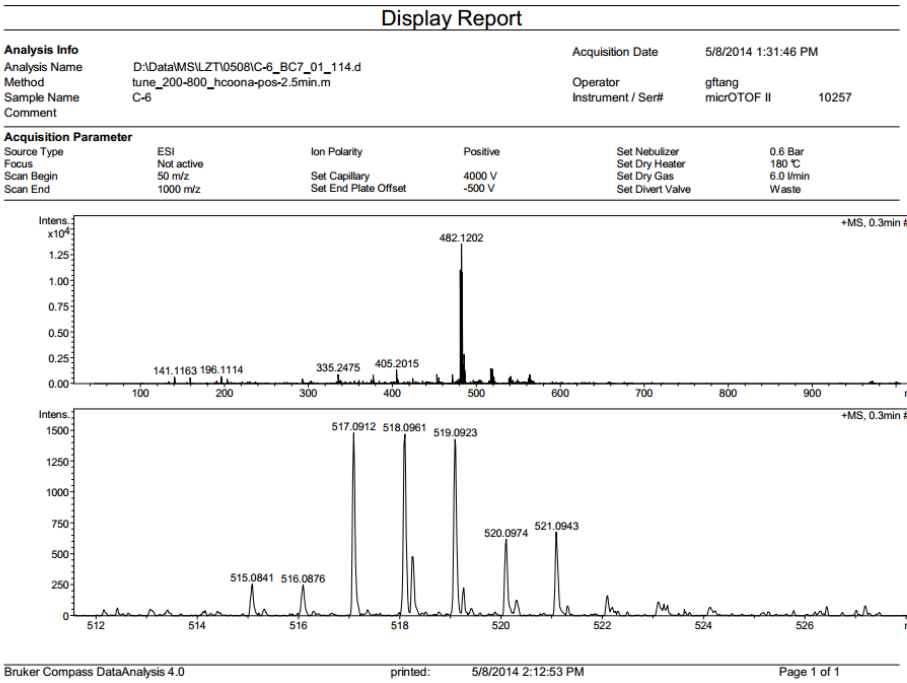

Fig. S48 Mass Spectrum of **C6**

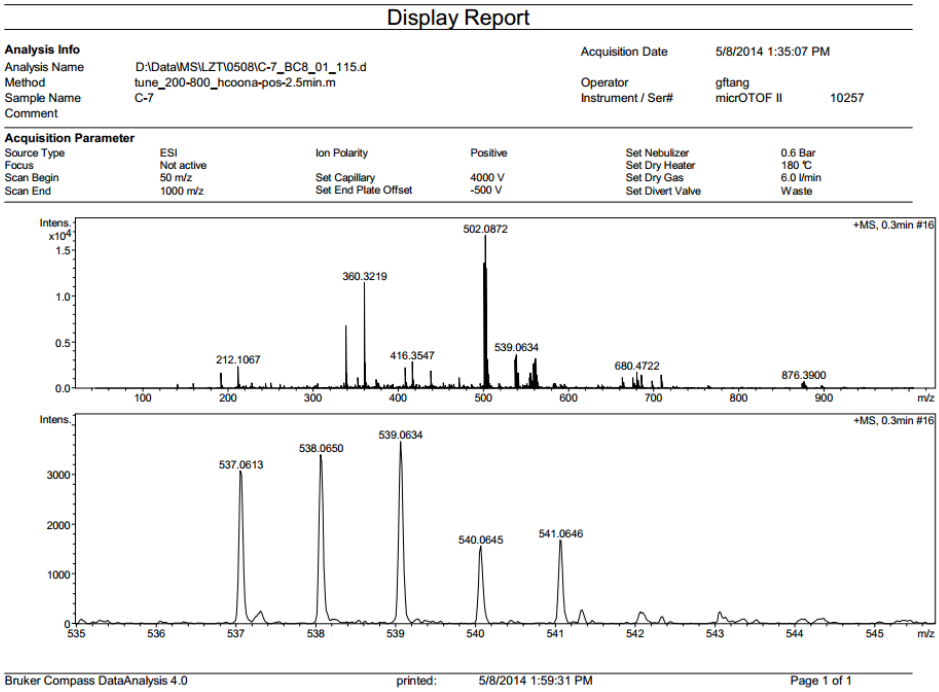

Fig. S49 Mass Spectrum of **C7**

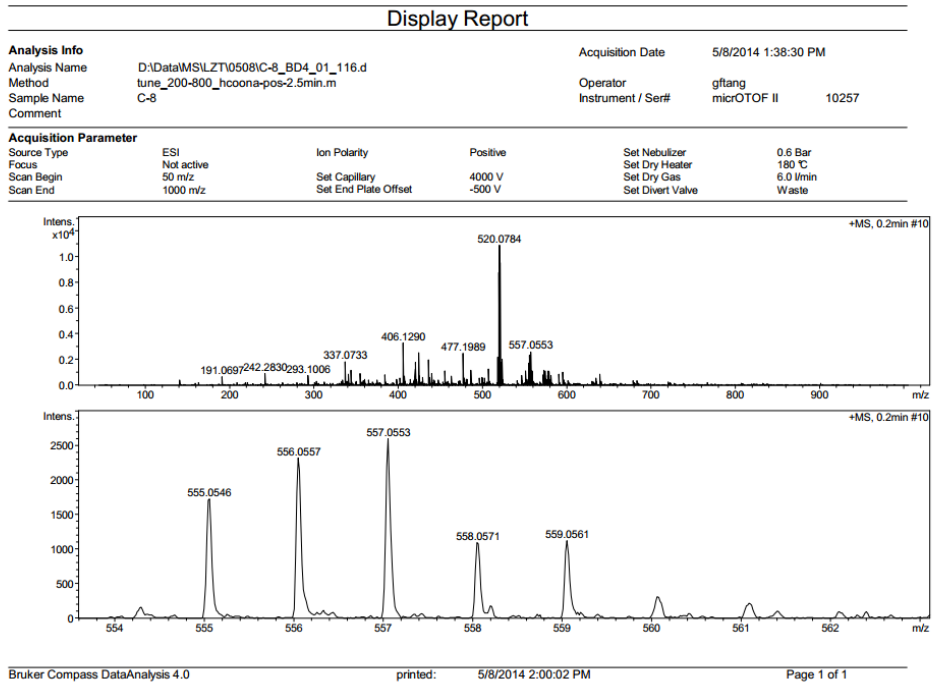

Fig. S50 Mass Spectrum of **C8**

Stabliltiy study

Stability of metal complex studied for cytotoxic analysis is always important. Therefore we perfomed stability analysis experiments for **C2, C3** and **C5** as model complexes using ^{1}H NMR spectroscopy in 10–15% D_2O–DMSO-d_6 mixture under room temperature at 0, 24, 48, and 72 h. No changes were obsereved in ^{1}H chemical shifts and also in peak number (Fig. S51 for **C2**, Fig. S52 for **C3** and Fig. S53 for **C5** below). It is concluded that **C2, C3** and **C5** are highly stable under these conditions.

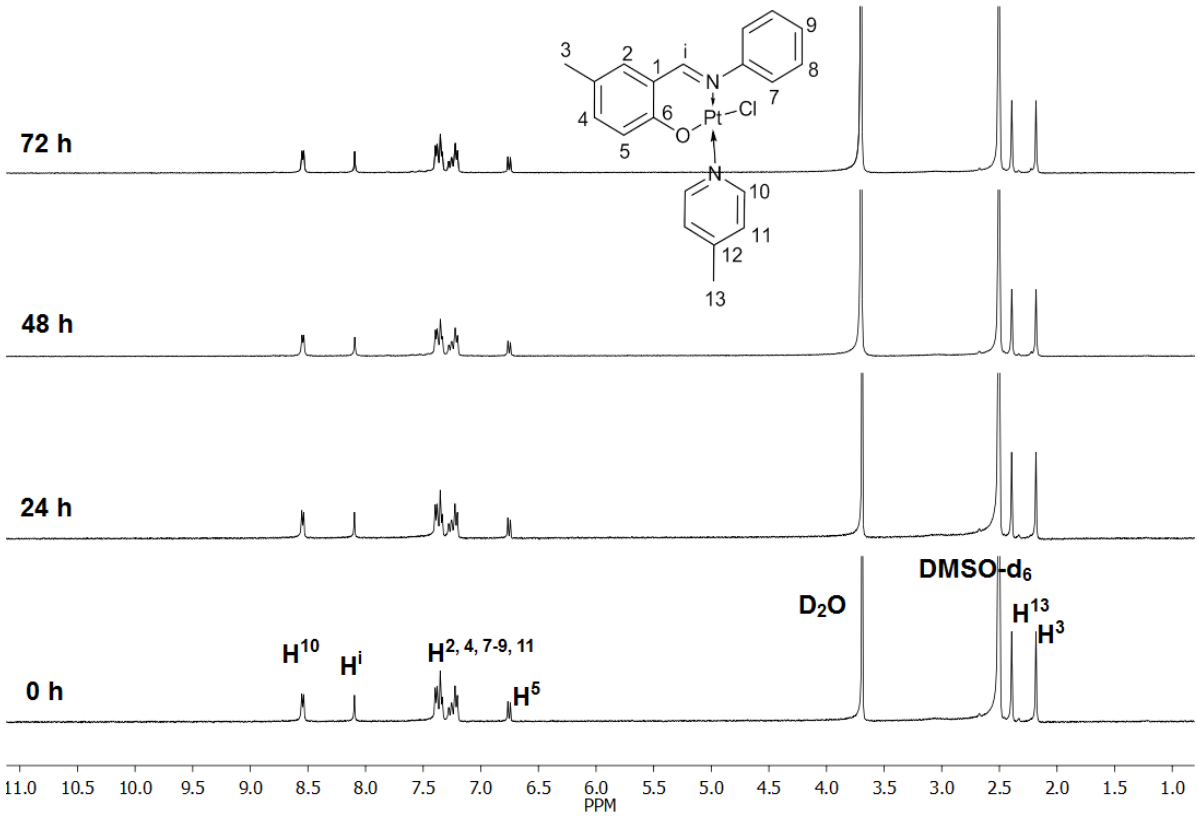

Fig. S51 Stability analysis of **C2** using ^{1}H NMR, taken in 15% D_2O–DMSO-d_6 at room temperature during (bottom to top) 0, 24, 48 and 72 h.

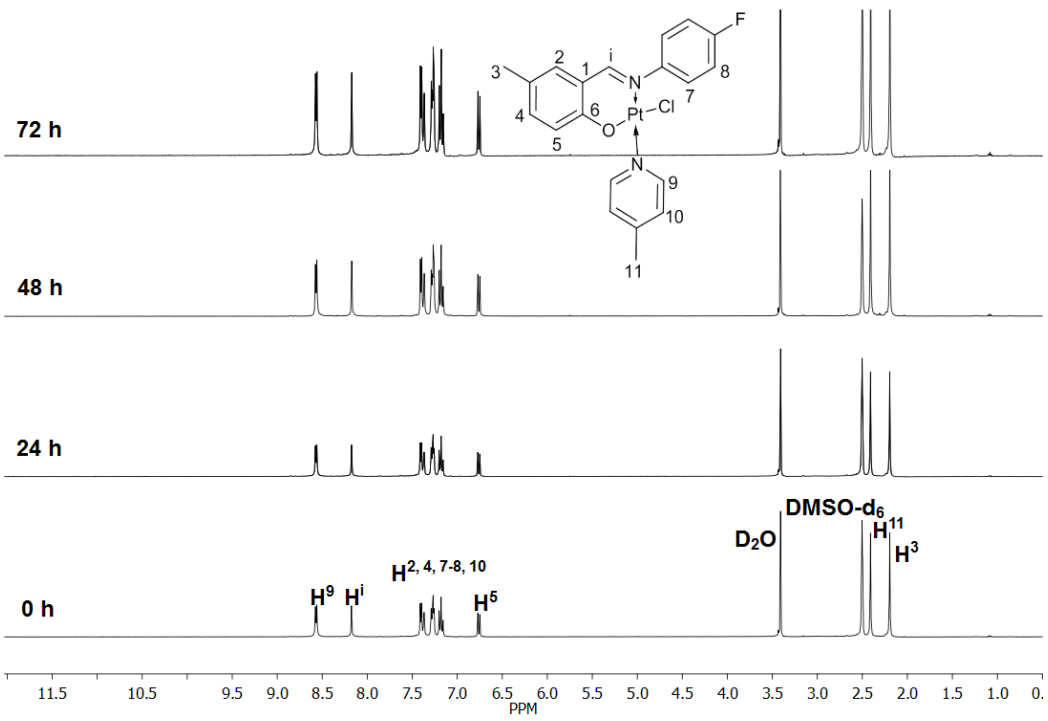

Fig. S52 Stability analysis of **C3** using ^{1}H NMR, taken in 10% D_2O–DMSO-d_6 at room temperature during (bottom to top) 0, 24, 48 and 72 h.

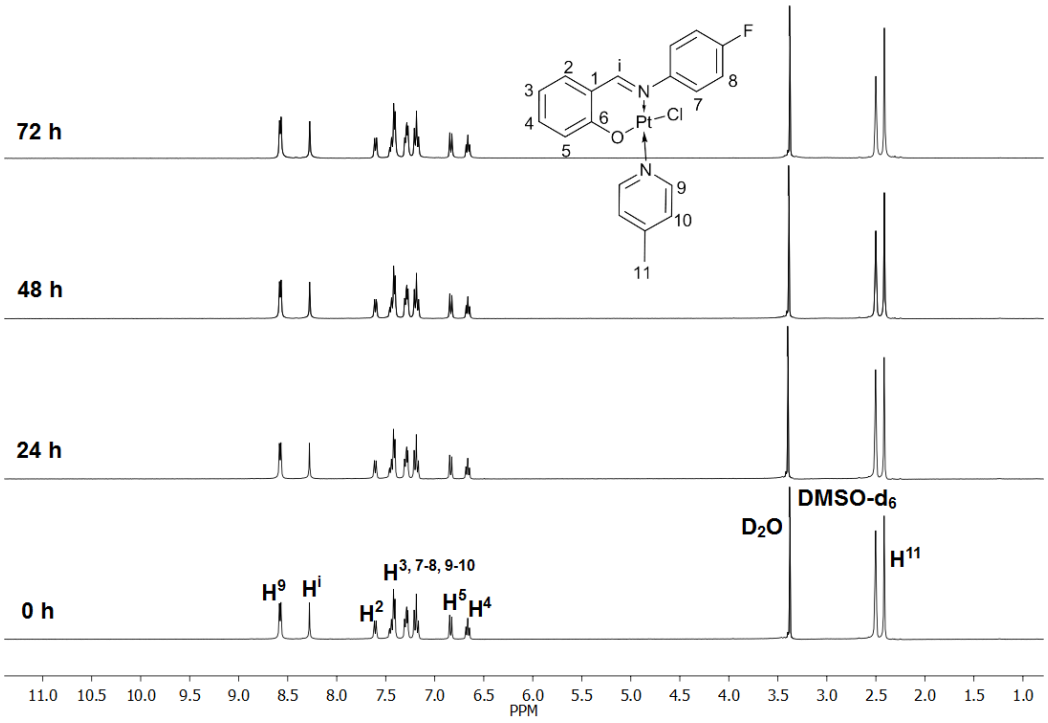

Fig. S53 Stability analysis of **C5** using ^{1}H NMR, taken in 10% D_2O–DMSO-d_6 at room temperature during (bottom to top) 0, 24, 48 and 72 h.

Single crystal structure study and refinement data of C1, C2 and C3

Table S1 data and structure refinement of the complex C1, C2 and C3

	C1	C2	C3
Empirical formula	$C_{18}H_{23}ClN_2OPt$	$C_{20}H_{19}ClN_2OPt$	$C_{20}H_{18}ClN_2OPt$
Formula weight	513.92	533.91	551.90
Temperature (K)	293(2)	233(2)	293(2)
Crystal system	Monoclinic	Monoclinic	Triclinic
Space group	P 21/c	P 21/c	P -1
Unit cell dimensions			
a (Å)	14.219(7)	13.766(2)	7.961(3)
b (Å)	11.945(6)	12.267(2)	10.420(4)
c (Å)	10.835(6)	11.094(2)	12.674(5)
α (°)	90	90	84.941(5)
β (°)	93.962(6)	93.872	74.687(5)
γ (°)	90	90	72.304(5)
Volume ($Å^3$)	1836.0(16)	1869.1(6)	966.0(7)
Z	4	4	2
Density (calculated) (mg/m^3)	1.859	1.897	1.897
Absorption coefficient (mm^{-1})	7.793	7.660	7.421
F(000)	992	1040	528
Crystal size (mm^3)	0.600 × 0.500 × 0.200	0.700 × 0.200 × 0.140	0.200 × 0.100 × 0.050
Theta range for data collection (°)	2.229 to 26.000	1.483 to 27.397	1.666 to 25.006
Index ranges	–17 ≤ h ≤ 17, –12 ≤ k ≤ 14, –12 ≤ l ≤ 13	–17 ≤ h ≤ 17, –15 ≤ k ≤ 12, –14 ≤ l ≤ 14	–4 ≤ h ≤ 9, –12 ≤ k ≤ 12, –14 ≤ l ≤ 14
Reflections collected	8007	12631	4009
Independent reflections	3582 [R(int) = 0.1028	4228 [R(int) = 0.0493]	3327 [R(int) = 0.0484]
Completeness to theta = 25.242° (%)	99.4	99.5	95.3
Absorption correction	Semi-empirical from equivalents	Semi-empirical from equivalents	Semi-empirical from equivalents
Max. and min. transmission	1.000 and 0.314	0.746 and 0.252	1.000 and -0.099
Refinement method	Full-matrix least-squares on F^2	Full-matrix least-squares on F^2	Full-matrix least-squares on F^2
Data / restraints / parameters	3582 / 0 / 212	4228 / 0 / 228	3327 / 12 / 237
Goodness-of-fit on F^2	1.041	1.054	1.094
Final R indices [I>2sigma(I)]	$R1^{[a]}$ = 0.0592, $wR2^{[b]}$ = 0.1491	$R1^{[a]}$ = 0.0444, $wR2^{[b]}$ = 0.1320	$R1^{[a]}$ = 0.0580, $wR2^{[b]}$ = 0.1699
R indices (all data)	$R1^{[a]}$ = 0.0674, $wR2^{[b]}$ = 0.1533	$R1^{[a]}$ = 0.0523, $wR2^{[b]}$ = 0.1385	$R1^{[a]}$ = 0.0655, $wR2^{[b]}$ = 0.1736
Extinction coefficient	n/a	n/a	n/a
Largest diff. peak and hole	4.420 and –2.775 $e.Å^{-3}$	1.763 and –2.859 $e.Å^{-3}$	2.342 and –3.095 $e.Å^{-3}$

[a] $R1 = \Sigma_{\text{all reflections}} |F_0 - F_c| / \Sigma_{\text{all reflections}} |F_0|$, [b] $wR2 = [\Sigma w(F_0^2 - F_c^2)^2 / \Sigma (w(F_0^2)^2)]^{1/2}$.

Packing plot of C1

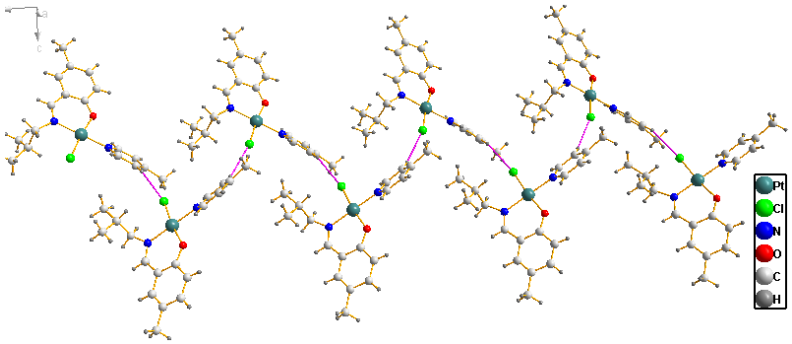

Fig. S54 1D array made by intermolecular bond between chloride attached to Pt center and H of the next molecule in **C1**

Packing plot of C2

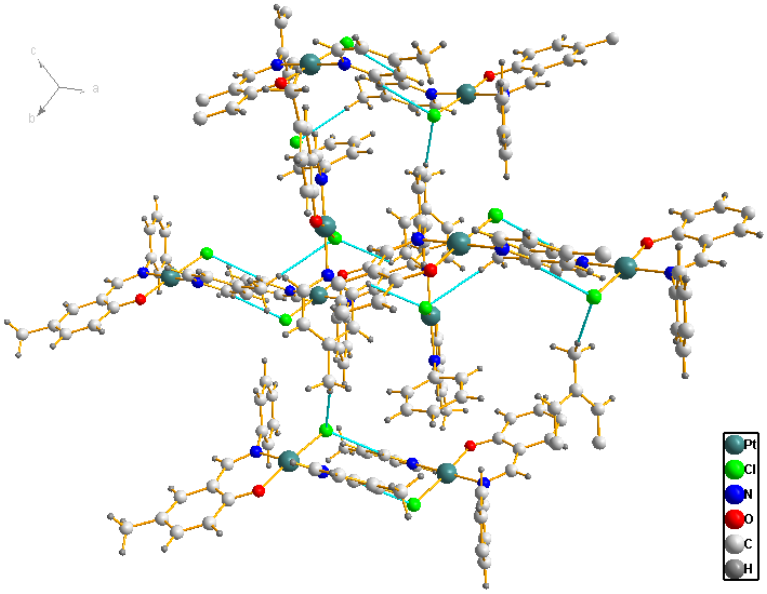

Fig. S55 3D arrangement of molecules in crystal packing; made by intermolecular bonds between chloride attached to Pt center and H of the next molecule (blue bonds) in **C2**

Packing plot of C3

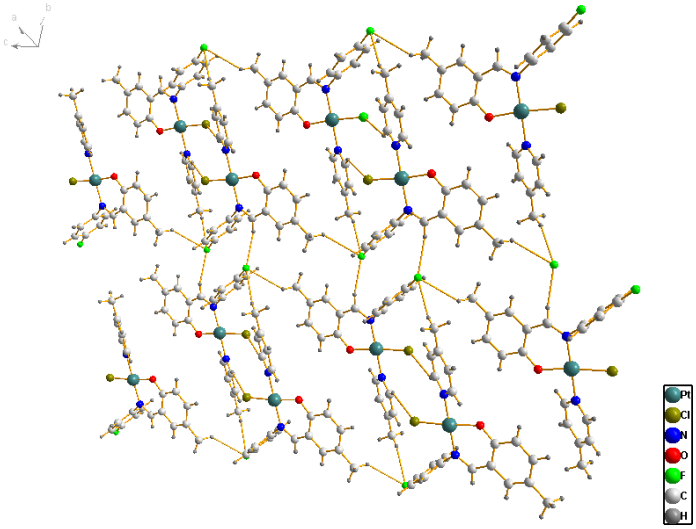

Fig. S56 3D arrangement of molecules in crystal packing; made by intermolecular bonds between chloride attached to Pt center and H of the neighbor molecule in **C3**